Defense Intelligence Reference Document

[redacted]

Acquisition Threat Support

6 April 2010

ICOD: 1 December 2009

DIA-08-1004-005

High-Frequency Gravitational Wave Communications

High-Frequency Gravitational Wave Communications

Prepared by:

(b)(3):10 USC 424

Defense Intelligence Agency

Author:

(b)(6)

Administrative Note

This product is one in a series of advanced technology reports produced in FY 2009 under the Defense Intelligence Agency, (b)(3):10 USC 424 Advanced Aerospace Weapon System Applications (AAWSA) Program. Comments or questions pertaining to this document should be addressed to (b)(3):10 USC 424;(b)(6), AAWSA Program Manager, Defense Intelligence Agency, ATTN: (b)(3):10 USC 424 Bldg 6000, Washington, DC 20340-5100.

Contents

Figures

High-Frequency Gravitational Wave Communications

Summary

- **Fourteen laboratory high-frequency gravitational wave (HFGW) generators (or transmitters) have been proposed in the past 45 years in peer-reviewed journal articles.**
- **The most promising laboratory HFGW generators are those that utilize very large numbers of sub-microscopic radiation elements.**
- **The Piezoelectric Approach to HFGW generation is best for the proof-of-concept test and the proposed IR-excited Molecules Approach is best for an operational communications HFGW transmitter.**
- **Ten different HFGW detectors (or receivers) have been proposed since 1978 and reported in peer-reviewed journal articles.**
- **Several different HFGW receivers can be utilized for communication, but the proposed Li-Baker detector (plans & specification development in Appendix B) shows the most promise (underlying concept in Appendix C). The Li-effect, upon which the Li-Baker detector is based, is not so new that it is untested in the literature. At least nine peer-reviewed research publications concerning the theory have appeared following the initial peer-reviewed article by Li, Tang and Zhao (1992).**
- **Because HFGW communications are carried on an extremely narrow beam directly through the Earth, there is a very low probability of interception.**
- **Theoretical results confirm that the Li-Baker detector is photon-signal limited, not quantum-noise limited—that is, the Standard Quantum Limit is so low that a properly designed Li-Baker detector can have sufficient sensitivity to observe HFGWs of amplitude $A \approx 10^{-32}$ m/m.**
- **Utilizing the IR-excited Molecules HFGW generator approach and the Li-Baker detector, the theoretical information-transfer rate over 7,000 km of distance, beamed directly through the Earth, is about 1.9×10^{6} bits per second.**
- **A means of propagating a Frequency Time Standard may be one viable early low-bandwidth application for HFGW communications.**
- **HFGW sources on the Earth, the Moon, and Mars may act as reference standards for interplanetary navigation, with the advantage that they cannot be shielded or shadowed by planetary masses. Plasma interference seen at planetary entry would be eliminated, and precise charting of Lagrangian points would be possible.**

1.0 Introduction

1.1 INTRODUCTION

Of the applications of high-frequency gravitational waves (HFGWs), communication appears to be the most important and most immediate. Gravitational waves have a very low cross section for absorption by normal matter, so high-frequency waves could, in principle, carry significant information content with effectively no absorption unlike electromagnetic (EM) waves. Multi-channel HFGW communications can be both point-to-point (for example, to deeply submerged submarines) and point-to-multipoint, like cell phones. HFGWs pass through all ordinary material things without attenuation and represent the ultimate wireless system. One could communicate directly through the Earth from Moscow in Russia to Caracas in Venezuela—without the need for fiber optic cables, microwave relays, or satellite transponders. Antennas, cables, and phone lines would be things of the past. A timing standard alone, provided by HFGW stations around the globe, could result in a multi-billion dollar savings in conventional telecom systems over ten years, according to the recent analysis of Harper and Stephenson (2007). The communication and navigation needs of future magneto hydrodynamic (MHD) aerospace vehicles, such as the MHD aerodyne (www.mhdprospects.com), which is high in electromagnetic interference, similar to plasma interference seen at reentry, would be another possible applications area for HFGW communications.

1.2 DEFINITION OF HIGH-FREQUENCY GRAVITATIONAL WAVES

Visualize the luffing of a sail as a sailboat comes about or tacks. The waves in the sail's fabric are similar in many ways to gravitational waves (GWs), but instead of sailcloth fabric, gravitational waves move through a "fabric" of space. Einstein called this fabric the "space-time continuum" in his 1915 work known as General Relativity (GR). Although his theory is very sophisticated, the concept is relatively simple. This fabric is four-dimensional: it has the three usual dimensions of space—east-west, north-south, and up-down—plus the fourth dimension of time. Here is an example: we define a location on this "fabric" (Einstein, 1916) as 5th Street and Third Avenue on the fourth floor at 9 AM. No one can see this "fabric," just as no one can see wind, sound, or gravity. Nevertheless, those elements are real, and so is this "fabric." If one could generate ripples in this space-time fabric, many applications would become available. Much like radio waves can be used to transmit information through space, gravitational waves could be used to perform analogous functions. Gravitational waves are the subject of extensive current research, which so far has focused on low frequencies. High-frequency gravitational waves, as defined by physicists Douglass and Braginsky (1979), are gravitational waves having frequencies higher than 100 kHz. Low-frequency gravitational waves (LFGWs), such as those detectable by interferometric GW detectors (for example, the Laser Interferometer Gravitational Observatory, or LIGO) are not applicable to communications due to their very long wavelengths, often thousands of kilometers in length and, even more importantly, the inability to generate them effectively in the laboratory. Furthermore LFGW detectors cannot detect HFGWs (Shawhan, P. S., 2004).

2.0 HFGW Communications

Consider the case of a single point-to-point two station full duplex communication system, as is represented in Figure 1. Such a system is often characterized as a single data link, and requires two transmitters, one at each end, and two receivers, one at each end. To avoid self-interference the link in one direction often uses a frequency of radiation different than the link in the opposite direction.

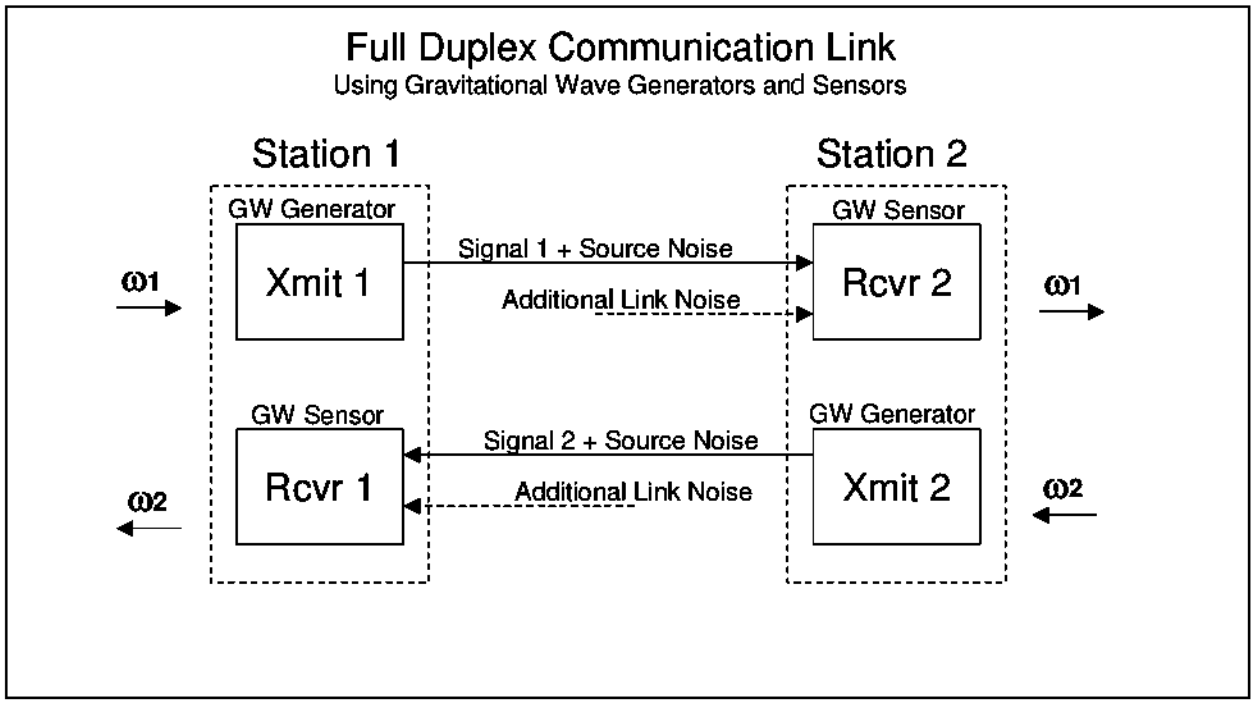

Figure 1. Communication Link Block Diagram

If one were to apply the emerging technology of gravitational wave control to such a link, one would use GW generators for the transmitters on each end, and GW sensors for the receivers at each end (Stephenson, 2009a). In the example shown in Figure 1, station 1 would have a GW generator transmitting at a frequency of ω_1 and a GW sensor sensitive to a frequency of ω_2, without being sensitive to a frequency of ω_1. Likewise, station 2 would have a GW generator transmitting at a frequency of ω_2 and a GW sensor sensitive to a frequency of ω_1, without being sensitive to a frequency of ω_2. This is the minimum functionality required to constitute a communication link. Signal strengths of the respective GW generators would need to be sufficient to overcome link loss, coupling losses, and noises sources. Signal to noise considerations and link budgets are covered in further detail in Section 3.1.

2.1 HFGW GENERATORS (TRANSMITTERS)

2.1.1 HFGW Generator Concepts

Several sources for HFGWs or means for their generation exist. The first generation means is the same for gravitational waves (GWs) of all frequencies and is based upon the quadrupole equation first derived by Einstein in 1918. A formulation of the quadrupole that is easily related to the orbital motion of binary stars or black holes,

rotating rods, laboratory HFGW generation, and so forth is based upon the "jerk" or shake of mass (time rate of change of acceleration) and is derived by Baker (2006) as

$$P = 1.76\times10^{-52}\,(2r\Delta f/\Delta t)^2 \text{ W} \qquad (1)$$

where P is the power of the GWs, W; r is the distance between two masses, m; Δf is a change in force, N; over the time interval Δt, s; that is, the jerk or shake of the two masses, such as the change in centrifugal force vector with time; for example, as masses move around each other on a circular orbit. Figure 2 describes that situation. Please recognize, however, that Δf need NOT be a gravitational force (see Einstein, 1918; Infeld quoted by Weber 1964, p. 97; Grishchuk 1974). Electromagnetic forces are more than 10^{35} larger than gravitational forces and should be employed in laboratory GW generation. As Weber (1964, p. 97) points out: "The non-gravitational forces play a decisive role in methods for detection and generation of gravitational waves ..." Equation (1) is also termed "quadrupole formalism" and holds in weak gravitational fields (well over 100 g's), for speeds of the generator "components" less than the speed of light and for r less than the GW wavelength. This last restriction may not really apply. Certainly there would be GW generated for r greater than the GW wavelength, but the quadrupole formalism might not apply exactly. For very small Δt, the GW wavelength, $\lambda_{GW} = c\Delta t$ (where $c \sim 3\times10^8$ ms^{-1}, the speed of light) is very small and the GW frequency v_{GW} is high. As a numerical example, r is choosen to be 10 m (convenient laboratory size, though usually greater than λ_{GW}), $\Delta f = 4\times10^8$ N; for example, the force produced by a large number of piezoelectric resonators and $\Delta t = 2\times10^{-10}$ s; equivalent to about a v_{GW} = 5 GHz jerk or shake frequency so that λ_{GW} = 6 cm and $P = 2.8\times10^{-13}$ W or 0.28 picowatts. Clearly a very small HFGW power is generated.

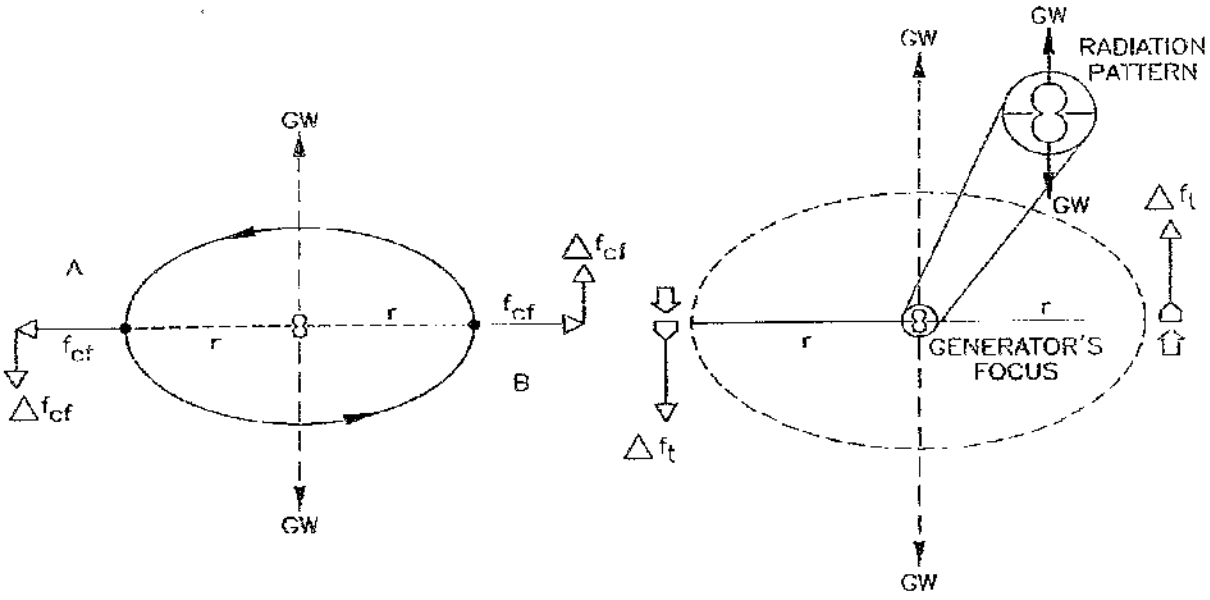

Figure 2. Change in Centrifugal Force of Orbiting Masses, Δf_{cf}, Replaced by Change in Tangential Force, Δf_t, to Achieve HFGW Radiation

One of the first suggested means for the laboratory generation of HFGWs was the so-called *gaser* analogous to the *laser* for light. Simply described (Halpern and Laurent,

1964), the gaser consists of a long rod of a material and microscopic parts of which can be excited by a means, such as electromagnetic (EM) radiation, to emit HFGWs. They utilize linearized theory to treat the interaction of a gravitational field with matter: "Application is made to the emission … of gravitons by microscopic systems such as molecules and nuclei." Grishchuk and Sazhin in early 1974 discussed the emission of gravitational waves by an electromagnetic cavity. In August of 1974 Chapline, Nuckolls and Woods suggested the generation of HFGWs by nuclear explosions. In this same regard Fontana suggested that the problem of efficient generation of HFGWs and pulses of gravitational radiation might find a reasonably simple solution by employing nuclear matter (Fontana and Baker, 2006; Fontana and Binder, 2009), especially isomers. A fissioning isomer not only rotates at extremely high frequency ($\sim 3.03\times10^{24}$ s^{-1}) according to the aforementioned references, but is also highly deformed in the first stages of fission (the nucleus is rotating and made asymmetric "before" fission). Thus one achieves significant impulsive forces (for example, 3.67×10^{8} N) acting over extremely short time spans (for example, 3.3×10^{-22} s). Alternatively, a pulsed particle beam, which could include antimatter, could trigger nuclear reactions and build up a coherent GW as the particles move through a target mass. The usual difficulty with HFGWs generated by nuclear reactions is the small dimensions of their nuclear-reaction volumes—that is, the small moment of inertia and submicroscopic radii of gyration (for example, 10^{-16} m) of the nuclear-mass *system*. Such a difficulty is overcome by utilizing small clusters of nuclear material, whose nuclear reactions are in synchronization; for example, through the use of a computer controlled logic system. Such nuclear-energized HFGW generators are currently very theoretical. Braginsky and Rudenko (1978) discussed the generation of gravitational waves in the laboratory and proposed a means utilizing small particles In 1981 Romero and Dehnen analyzed the generation of gravitational radiation in the laboratory also utilizing a linear array of piezoelectric crystals that will be analyzed in more detail in Section 2.1.3. In 1988 Pinto and Rotoli presented a paper on the laboratory generation of gravitational waves at the *Italian Conference on General Relativity and Gravitational Physics*. Another Italian, Giorgio Fontana (1998), suggested that the possibility of emission of high frequency gravitational radiation from junction between d-wave and s-wave superconductors. Kraus (1991) proposed that gravitational-wave communication might be possible in the *IEEE Antennas & Propagation* magazine. At the first HFGW Working Group Conference at the MITRE Corporation in 2003, Grishchuk analyzed electromagnetic generators and detectors of gravitational waves. At that same Conference Valentin Rudenko presented a paper on the optimization of parameters of a coupled generator-receiver for a HFGW Hertz experiment. At the second HFGW Working Group Conference in Austin, Texas, in 2007, Kolosnitsyn and Rudenko presented another paper on the generation and detection of the high-frequency gravitational radiation in a strong magnetic field. In 2007, and more recently this year, a new type of HFGW generator/detector and mirror system based on thin, type I superconducting films was proposed by R. Chiao, S. Minter, and K. Wegter-McNelly (2007; 2009a,b). Therefore it is evident that a number of devices for the laboratory generation of HFGWs have been proposed including the aforementioned gaser (as has been mentioned, was first proposed by Halpren and Laurent in 1964, some 45 years ago) discussed by Fontana and Baker (2003); as well as an actual laser generator of HFGWs as discussed by Li and Li (2006). Finally a rather practical laboratory HFGW generator, which may be appropriate for the initial proof-of-concept test, is one utilizing off-the-shelf components such as magnetron energized piezoelectric crystals or Film Bulk Acoustic Resonators or FBARs has been analyzed in Woods and Baker, (2005) and Baker, Woods and Li (2006).

The *figure of merit* for a HFGW generator is given explicitly by Baker, Woods and Li (2006). This Figure of merit can be extended by considering other effects since in the laboratory the force change could not even approach those of the celestial sources. It would seem that the magnitude of any laboratory generated GWs could be best increased (1) by utilizing electromagnetic forces rather than gravitational, (2) by increasing the distance between the gravitational radiators, (3) by increasing the GW frequency (that is, reducing Δt) and especially (4) by developing a large number of in-phase system elements. This last effect enters as the square of the number of elements, N , as proved using General Relativity analyses by Dehnen and Romero–Borja's analyses (Romero and Dehnen, 1981; Dehnen and Romero, 2003). Such N^2 dependence also may be the key to successful laboratory generation of GWs, especially HFGWs. In that regard, recent proposal by Woods (Woods and Baker, 2009; Black and Baker, 2009)) propose the use of infrared-energized atomic nuclei, electrons and or molecules, which have a very large N, contained in a stack of N waveguide rings (Patents Pending). The distance between GW radiators may be proportional to the GW wavelength in that it may have a limit that is less than or equal to a GW wavelength. The wavelength is inversely proportional to the GW frequency. Thus *given some value* for the proportional constant, say unity or the distance between radiators equal to one GW wavelength, the GW frequency cancels out. As already noted it is important to take advantage of square of the number of in phase elements for useful laboratory HFGW generation. If the elements are sliced in one dimension (the dimension along the axis of HFGW generation) in order to increase the number of elements, then the change in force per element will be inversely proportional to the number of elements. For example, if the elements are sliced into one hundred separate pieces, then each piece will have one hundredth of the force of the unsliced element. Essentially, f = ma and it is assumed that the acceleration of the element was the same after the split as before. This result also follows Equation (8), page 17 in Baker, Stephenson and Li (2008b) and if there were 100 splits of an FBAR, then the power to an individual slice, P and its mass, m would be both one hundredth of their un-split value and the square root of their product would again be one hundredth. The frequency of the split elements may be a higher value -- but the attendant increase in GW power proportional to the square of the higher frequency and the decrease in power due to a smaller distance between tracks (assuming that the distance between tracks is one GW wavelength, which would be smaller) would cancel and there would be no net effect on HFGW amplitude. It is concluded, therefore, that in this *particular special situation* the amplitude of the generated HFGWs is proportional to the number of in-phase elements, N (not the square). In any event a large number of elements for a given HFGW-generator length can be best realized by reducing the size of the individual elements to submicroscopic size (as discussed in U. S. Patent Number 6,784,591).

In the case of HFGW generation for communications applications, it is important to relate the amplitude of a GW, A, with the power, P, or more exactly with the GW flux, F_{GW}, in Wm^{-2}. For a viable communications link, the HFGW amplitude, A, must be large enough to be detected at the HFGW receiver. From Appendix B of Baker, Woods and Li (2006),

$$A = 1.28\times10^{-18} \left(F_{GW}/v_{GW}\right)^{1/2} \text{ m/m} \qquad (2)$$

where A has the dimensionless value of spacetime strain or m/m and v_{GW} is the GW frequency s^{-1}. Following the proceeding numerical example we will concentrate the HFGW on a diffraction-limited area of 4×10^{-3} m^2 or 0.004 m^2 for a HFGW flux of

$(2.8\times10^{-13})/(4\times10^{-3}) = 7\times10^{-11}$ Wm^{-2}. Thus A = 2×10^{-33}. It is an extremely small HFGW amplitude, but possibly a detectable signal.

2.1.2 Alternative Approaches

There are several alternative approaches to the laboratory generation of HFGWs developed over the past 45 years as discussed in the preceding Section 2.1.1. They can be categorized as EM-cavity generated, nuclear-energy generated, superconductor-generated, laser-impact generated and energized microscopic & submicroscopic-particle generated HFGWs. Of these categories the last category appears to be the most promising for early deployment in HFGW communications systems. Furthermore, one embodiment of that category: the Magnetron-energized FBARs generator, utilizing off-the-shelf equipment, would seem the most useful for proof-of-concept tests. For a practical, operational communications system HFGW generator (transmitter) the strong dependence of HFGW generator's power on the number of radiating elements, *N*, recommends a system utilizing molecular elements as suggested by Braginsky and Rudenko (1978) or using Infrared (IR)-energized pentane molecules in a stack of circular waveguides as proposed by Woods and Baker (2009). The Magnetron-energized FBARs and the IR-energized pentane will be considered in the next-following sections.

2.1.3 Piezoelectric Approach

Let us consider the 1.8×10^{8} cell-phone film bulk acoustic resonators or FBARs, 10,000 Microwave-Magnetron, proof-of-concept laboratory HFGW generator. Assuming a 10 μm distance or margin between the 100 μm square conventional FBARs, the overall length of the laboratory generator will be 110 × (10^{-6} m) × (1.8×10^{8} elements) = 19.8 km. It will have a total HFGW power of 0.066 W and for a distance out from the last in-line, in-phase FBAR element of one HFGW wavelength (6.1 cm) it will have a flux of 3.53 Wm^{-2}, yielding a HFGW amplitude there of A = 4.9×10^{-28} m/m. By the way, the inline set of FBAR elements also produces a more needlelike radiation pattern of HFGWs so that the flux and resulting A may even be larger. Although the frequencies may be different analyses (2003), one can extrapolate approximately from the results of Dehnen and Romero–Borja's analyses in which the angle of the needle-like radiation pattern is inversely proportional to the square root of the product of the distance between the radiators (the width between FBAR bands or tracks) and *N*. The distance for the system discussed here is 6.1 cm and for Dehnen's system 0.00001 m, for a factor of 6,100 and *N* differs by $(1.8\times10^{8})/(5\times10^{7}) = 3.6$ for a product of 2.2×10^{4} and the inverse of the square root is 6.7×10^{-3}. Using the result from Dehnen's paper (Equation (4.51), page 12) of a needle half angle of 1.7 degrees we would extrapolate to 0.0115 degrees or very approximately 2×10^{-4} radians. Since there is no longer the constraint to the use of rudimentary off-the-shelf components as there was for the proof-of-concept apparatus, the specially designed submicroscopic elements can be manipulated. First, they will be staggered into two bands or tracks of 100 rows each or 110 × 100 μm = 1.1 cm wide bands of FBARs a wavelength or 6.1 cm apart. The rows will be staggered by displacing adjacent rows in the bands by 1.1 μm. Thus the overall length will be reduced to 198 m. Second, the 100 μm length of each FBAR element can be sliced, along the direction of travel of the HFGW build up, into one-hundred 1 μm wide slices (exhibiting 0.1 μm margins). The staggered row displacements are now reduced to 11 nm. The overall length will be reduced to about 198 cm. Concentrating the 10 MW power to each of these 1.1 cm wide bands may prove to be difficult. Thus, as an example, the continuous-wave Magnetrons will be replaced by a pulsed microwave source having

one-microsecond-long pulses one second apart. The required average power for each FBAR band will now be 10 W. As a practical nanotechnology limit, the slice width can be reduced by two orders of magnitude to 10 nm. This would also require that the row displacements would be 110 pm (we are now into atomic if not sub-atomic dimensional changes). The overall length could be reduced to about 2 cm or the amplitude of the HFGWs could be increased to $A = 4.9\times10^{-26}$. In this latter case the average energizing microwave power applied to each band would need to be increased to 1 kW. A preferred compromise in this apparent nano-technology limit might be to reduce the HFGWs generator's length to about 20 cm and increase the HFGW amplitude A to 4×10^{-27} m/m.

The complementary approach to optimizing a practical HFGW generator is to increase the force produced by each element without increasing the required power (that is, increasing element efficiency). This was initially done using the modern light-weight piezoelectric FBARs rather than the heavy 10-gram crystals considered by Dehnen and Romero-Borja that were of 1981 vintage. Special designs of FBAR-like elements for optimum force-generation efficiency will improve the HFGW generator performance beyond that for the usual cell-phone FBAR designs. Another approach to element design is to utilize nano-size lasers whose targets are the force-generating elements (Li and Li, 2006). Utilization of myriads of nano-size lasers would generate high-frequency HFGW pulses as noted in U. S. Patent Number 6,784,591. Thus there are a number of opportunities to enhance HFGW generation performance, utilizing special element designs, either by reducing the generator size or increasing the generated HFGW amplitude or both.

2.1.4 Infrared-Excited Molecules Approach

The very theoretical IR-generated HFGWs suggested by Woods and Baker (2009) have significant promise. If one has a standing wave in a waveguide ring and excites it properly, then one will have a GW source at its center, as shown in Figure 3. The GW flux produced at its center is proportional to the n submicroscopic particle pairs (in this case pentane molecule pairs) in each ring. There is no n^2 buildup, but there is an n buildup. If one has a stack of N plates of rings, which are excited in sequence at light speed as a generated, growing as a GW passes by, then one has an nN^2 buildup in GW flux.

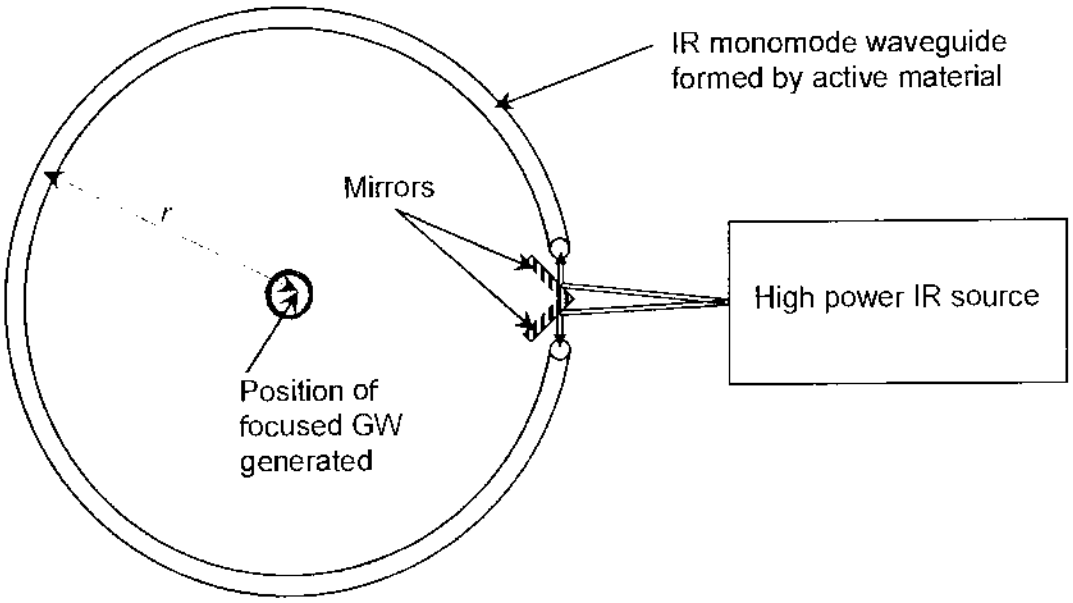

Figure 3. Circular Resonator Geometry Using Infrared Excitation

Analogous to Figure 2, we see in Figure 4 the radiation pattern for a pair of orbiting masses.

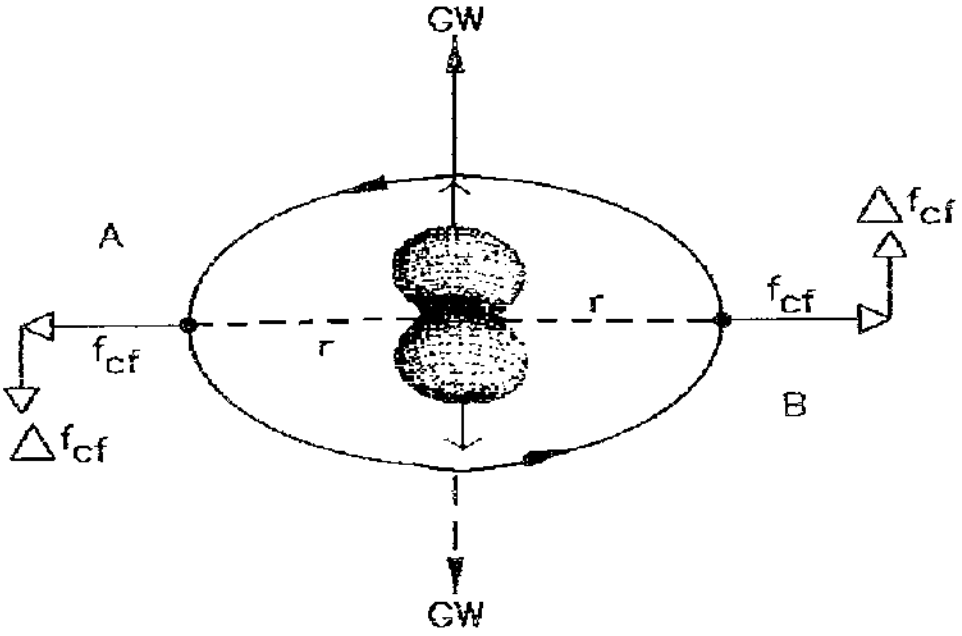

Figure 4. Radiation Pattern Calculated by Landau and Lifshitz (1975)

Next consider a number N of such orbit planes stacked one on top of another with the gravitational-wave (GW) radiation growing flux (Wm^{-2}) proportional to N^2 as the GW moves up the axis of the N orbit planes as in Figure 5.

The stack of orbital planes are no replaced by a stack of *N* plates each containing *n* molecules in each waveguide ring as exhibited in Figure 6. Now there is a HFGW wave moving up the axis of the rings (or normal to the waveguide plates) and increasing in strength according to the product nN^2.

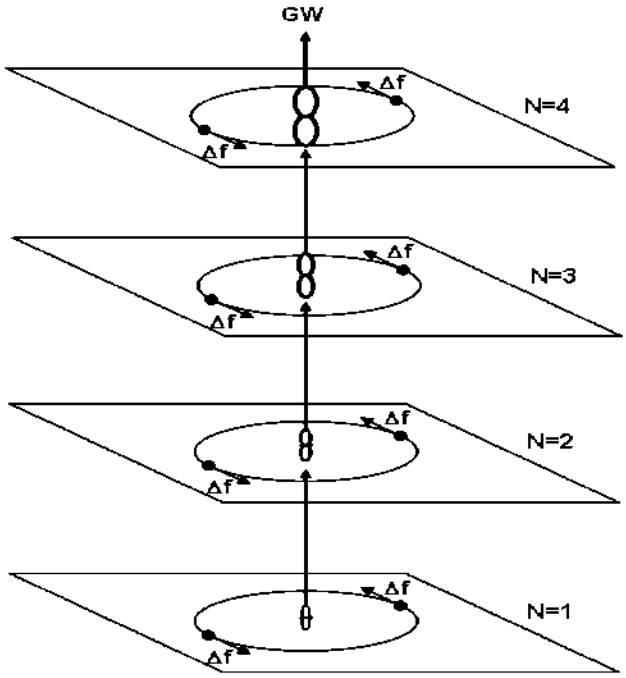

Figure 5. GW Flux Growth Analogous to Stack of N Orbital Planes

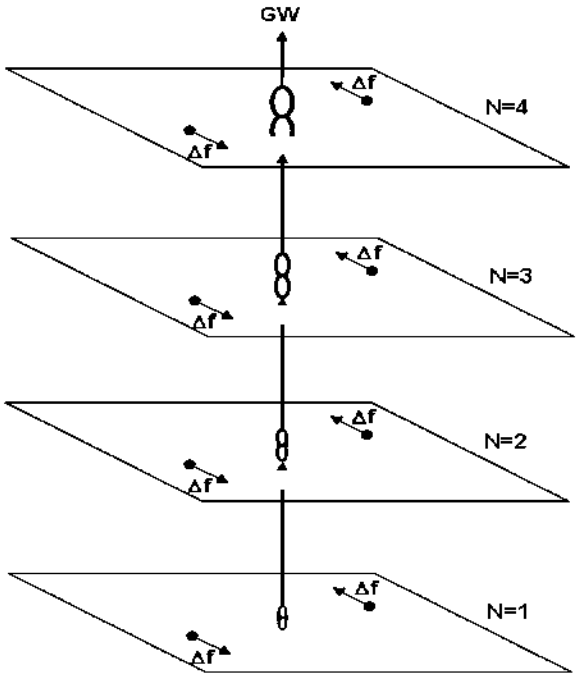

Figure 6. Stack of Circular-Wave-Guide Plates With Typical Molecule Jerks, Δf's

One should consider the IR rings in more detail. As calculated, the IR wavelength is about 2.5×10^{-6} m. The IR waveguide has a cross-sectional area radius of $\lambda/4$ in order for it to be a monomode (lowest order mode) so that the phase doesn't change across the waveguide. Thus the cross-sectional area of each IR ring is $\pi \times (2.5\times10^{-6}\ \text{m}/4)^2 = 1.23\times10^{-12}\ \text{m}^2$ and its diameter is 1.25×10^{-6} m. The volume of each 100-m radius nano-size toroidal ring is $2\pi \times (100) \times (1.23\times10^{-12}) = 7.7\times10^{-12}\ \text{m}^3$. The mass density of pentane is divided by its molecular mass and that gives the density of jerkable masses of $6.3\times10^{28}\ \text{m}^{-3}$. Thus the number of jerkable mass pairs, *n*, in a 100 m radius circular wave guide $2n = (6.3\times10^{28}) \times (7.7\times10^{-12}) = 4.85\times10^{17}$ submicroscopic "particles" or potentially jerkable masses or $n = 2.45\times10^{17}$ mass pairs. According to Table 1 of Woods and Baker (2009) for pentane $P_i = 4.62\times10^{-16}$ W. Thus the flux at one meter distance for all of the mass pairs in a single ring from Equation (8) of Black and Baker (2009) is $n \times (0.01146) \times P_i = 1.29\ \text{Wm}^{-2}$. It should be recognized that the axes of the opposite pentane molecules jerk (in response to the EM wave) may not be anti-parallel and tangential to the circular waveguides. On the other hand, the radiation pattern for the HFGW exhibits some omni-directional form, as shown in Figure 7, so significant HFGW radiation will be directed along the axis of the stack of circular waveguides (normal to the plates) and the HFGW will build up.

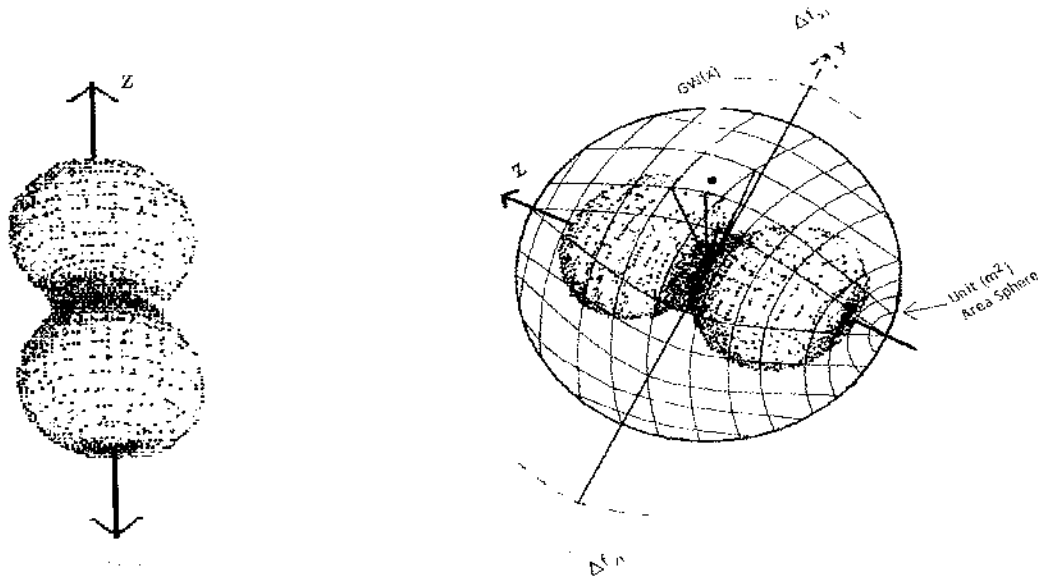

Figure 7. Omni-Directional Nature of the HFGW Radiation Pattern

Next consider a more convenient laboratory arrangement for the rings. The ring radius is reduced to one meter, but set up 100 rings, concentrically (side by side concentric rings in the same plane or plate) with an average radius of the one meter. The reduced radius drops the P_I by $(100)^2$ to 4.62×10^{-20}, but because of the 100 concentric rings the $n = 4.85\times10^{17}/2$ remains the same. Thus the flux for a single "plate" of concentric rings is only reduced by 10^4 to 1.29×10^{-4} Wm^{-2}. Now stack some 10^6 of these 1.25×10^{-6} *m* thick plates on top of one another. Thus a 1.25 m high stack, barrel or cylinder as described in Baker (2001) is created. In this case, as shown in Figure 6, $N = 10^6$ and the N^2 law can be applied. Thus a HFGW total flux of 1.29×10^8 Wm^{-2} in a very narrow beam will be generated by the stack. Of course (as pointed out in Woods and Baker (2009)) caution needs to be taken on how much power is fed to each ring. One possible arrangement is to feed the output of one ring to the input of the next. The problem here is that the source won't have a long enough coherence length, even if the attenuation of the IR doesn't kill the power after a ring or two. To avoid this, from one source the available energizing power could be divided equally between all the rings and fed to them up the stack or cylinder at the speed of light. The practical difficulties would be how to drive them all in correct phase, but it is a challenge for future research in the IR-ring approach.

For an operational 50,000Å infrared (IR), 12.5 meter long, 10-meter radius (10^4 concentric rings per plate so $P_I = 1.29\times10^2$ Wm^{-2} and 10^7 plates) cylindrical HFGW generator (Woods and Baker, 2009), the flux at a one-meter distance from the generator is, according to Table 1 of Black and Baker (2009) for $N = 10^7$, $(1.146\times10^{12}) \times (1.29\times10^2) = 1.48\times10^{14}$ Wm^{-2} (very large, but with a very narrow 2.3×10^{-4} radian half-power-point needle beam). The required generator power can be reduced by utilizing pulsed HFGWs. Suppose that the distance between the generating or transmitting device and the detecting or receiving device is a little more than an Earth's equatorial radius, or $\sim 7\times10^6$ meters. At this distance, 7,000 km, the flux of the

received signal, S, is $(1.48\times10^{14})/(7\times10^{6})^2$ = 3 Wm^{-2}, more than adequate for an effective communication system.

With this configuration, the width of the needle-like, narrow HFGW beam at the receive end is $(2.3\times10^{-4}) \times (7\times10^{6})$ = 1.6 km, and multiple HFGW carrier frequencies can be used, so the signal is very difficult to intercept, and is therefore useful as a low-probability-of-intercept (LPI) signal, even with widespread adoption of the technology. From Equation (2) the amplitude A of the HFGW at 7,000 km with the HFGW frequency (twice the IR frequency of $v_{GW} = 1.2\times10^{14}$ s^{-1}) given by: $A = 1.28\times10^{-18}\ (S/v_{GW})^{1/2} = 1.8\times10^{-32}$ (in dimensionless units or m/m), which would be detectable by the currently designed Li-Baker HFGW detector. Since the exact frequency and phase of the HFGW signal is known (unlike the stochastic relic HFGWs, for which the Li-Baker detector was designed), a much more sensitive, optimized HFGW detector will likely be developed.

As shown in Figure 8, from Grishchuk (2008), there will be negligible relic HFGW noise at the IR HFGW generator's frequency of 1.2×10^{14} s^{-1} and no other cosmic sources at these frequencies are currently hypothesized. Prior to the proof-of-concept test, one can assume a noise figure at the Li-Baker detector of 10^{-8} Wm^{-2}.

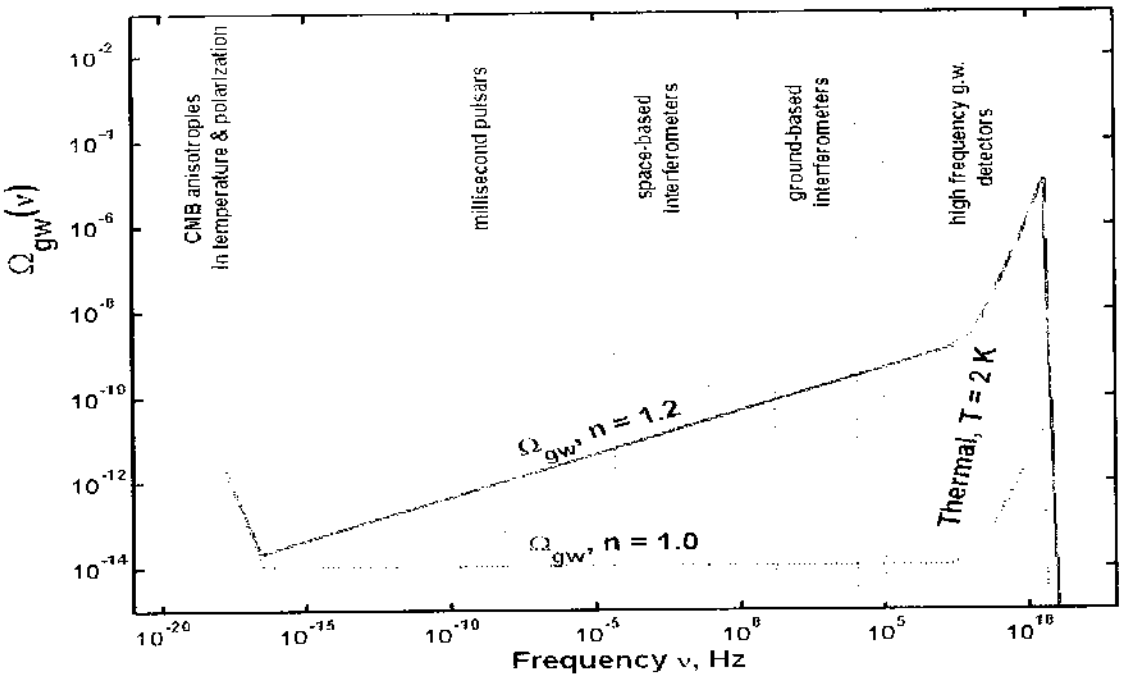

Figure 8. Predicted Relic GW Energy Density as a Function of Frequency

2.2 HFGW DETECTORS (RECEIVERS)

2.2.1 Alternative Approaches

One of the first suggested means for the detection of HFGWs concerns electromagnetic detectors (Braginsky, et al. 1974 and Braginsky and Rudenko, V, 1978). Then Pegoraro, et al. (1978) suggested the use of tuned resonant chamber HFGW detectors. Rudenko and Sazhin in 1980 proposed a Laser interferometer as a gravitational wave detector (somewhat similar to the current Japanese approach). In 1995 Tobar characterized multi-mode resonant-mass HFGW detectors and three years later in 1998 (Ottaway, et al.) proposed a compact injection-locked Nd:YAG laser for HFGW detection. And in 1999 Tobar suggested, microwave parametric transducers for the next generation of resonant-mass gravitational wave HFGW detectors.

In the past few years, HFGW detectors have been fabricated at *Birmingham University*, England, *INFN Genoa*, Italy and in Japan. These types of detectors may be promising for the detection of the HFGWs in the GHz band (MHz band for the Japanese) in the future, but currently, their sensitivities are orders of magnitude less than what is required for the detection of high-frequency relic gravitational waves (HFRGWs) from the big bang. Such a detection capability is to be expected, utilizing the Li-Baker detector (please see Appendix B for Plans & Specifications development). Nevertheless, all four candidate detectors; plus, possibly, the use of superconductors (Li and Baker, 2007) should be analyzed for possible military applications. The Li-Baker HFGW detector was invented by R. M L Baker, Jr. of Transportation Sciences Corporation, California and patented in P. R. China (Baker, 2001). Based upon the theory of Li, Tang and Zhao (1992) termed the Li-effect, the detector was proposed by Baker during the period 1999-2000, a patent for it was filed in 2001, subsequently granted (Baker, 2001), and preliminary details were published later by Baker, Stephenson and Li (2008a). This detector was conceived to be sensitive to relic HFGWs (HFRGWs) having amplitudes as small as 10^{-32} to 10^{-30}.

The *Birmingham University* HFGW detector measures changes in the polarization state of a microwave beam (indicating the presence of a GW) moving in a waveguide about one meter across (see Figure 9). Also see Cruise (2000), Ingley and Cruise (2001) and Cruise and Ingley (2005). It is expected to be sensitive to HFGWs having spacetime strains of $A \sim 2 \times 10^{-13}\ (\mathrm{Hz})^{-1/2}$, where Hz is the GW frequency, and as usual A is a measure of the strain or fractional deformation in the spacetime continuum (dimensionless m/m).

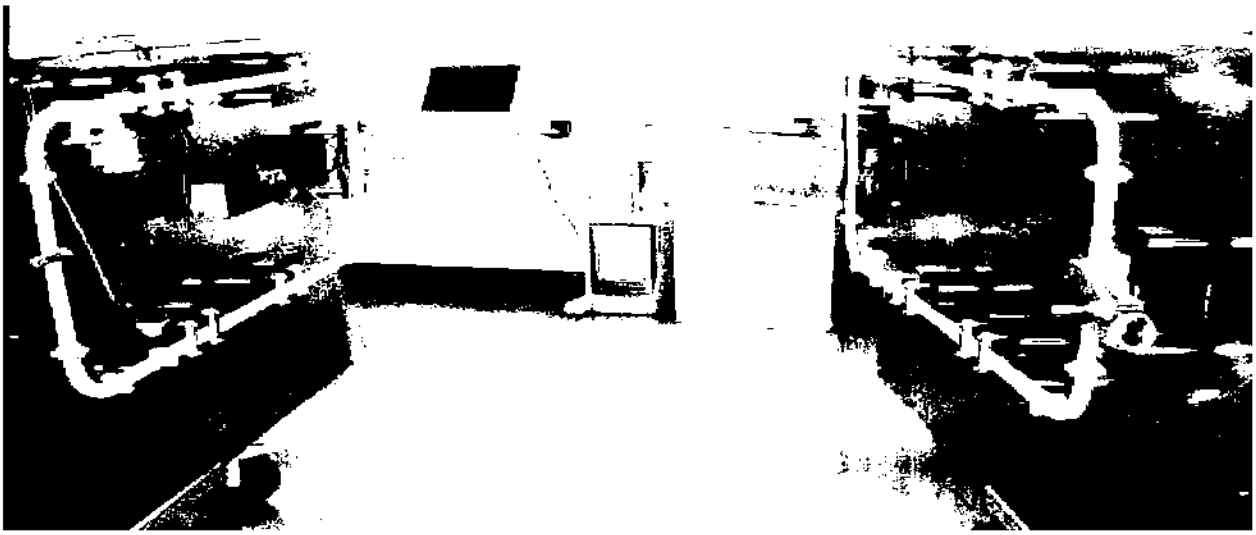

Figure 9. Birmingham University HFGW Detector

The *INFN Genoa* HFGW resonant antenna consists of two coupled, superconducting, spherical, harmonic oscillators a few centimeters in diameter (see Figure 10). The oscillators are designed to have (when uncoupled) almost equal resonant frequencies. In theory, the system is expected to have a sensitivity to HFGWs with size (fractional deformations) of about $\sim 2\times10^{-17}$ $(Hz)^{-½}$ with an expectation to reach a sensitivity of $\sim 2\times10^{-20}$ $(Hz)^{-½}$ (Bernard, Gemme, Parodi, and Picasso (2001); Chincarini and Gemme. (2003)). As of this date, however, there is no further development of the INFN Genoa HFGW detector.

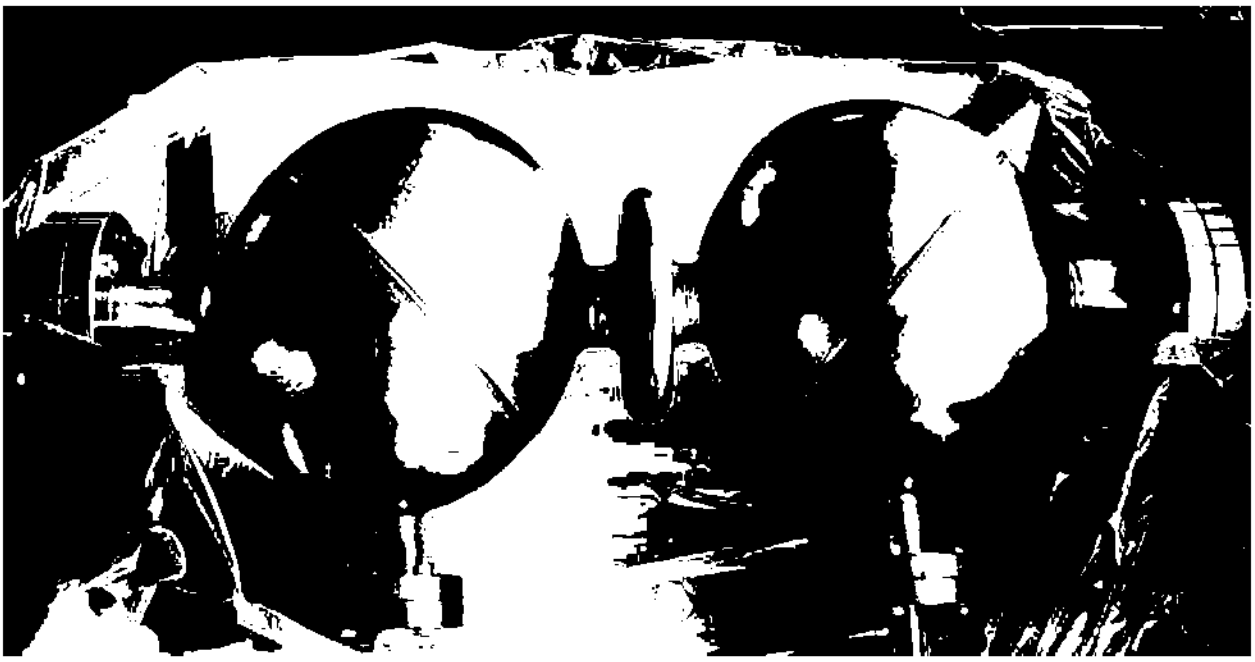

Figure 10. INFN Genoa HFGW Detector

The Kawamura 100 MHz HFGW detector has been built by the *Astronomical Observatory of Japan*. It consists of two synchronous interferometers exhibiting an arms length of 75 cm. Please see Figure 11. Its sensitivity is now about 10^{-16} $(Hz)^{-½}$

According to Cruise (2008) of Birmingham University its frequency is limited to 100 MHz and at higher frequencies its sensitivity diminishes. In the case of the Infrared-excited molecules approach, on might employ a variant of the Robinson Gravitational Wave Background Telescope for the receiver or detector (Yoon, et al., 2006). It is a bolometric large angular scale Cosmic Microwave Background (CMB) polarimeter, but might possibly be modifiable for direct HFGW detection.

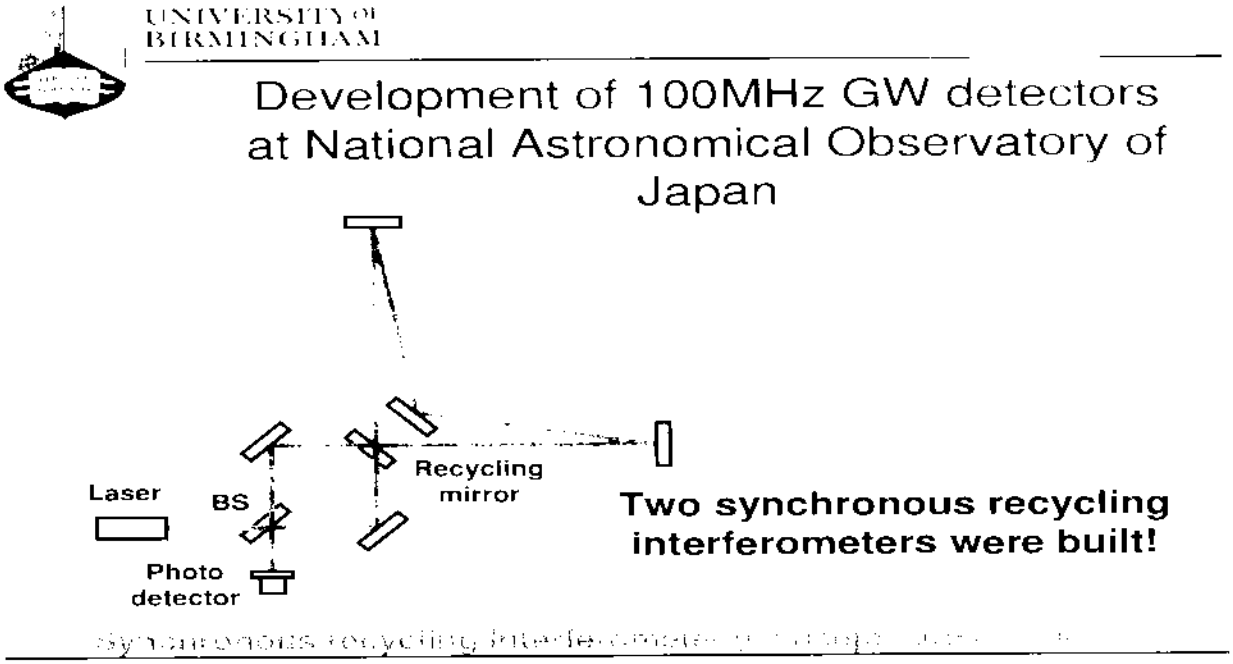

Figure 11. The National Astronomical Observatory of Japan 100 MHz Detector

2.2.2 Concept (Li-Effect)

The Li-Effect was first published in 1992 and subsequently, some nine peer-reviewed papers have been published concerning it including a capstone paper, Li, et al. (2008) included as Appendix C. The Li-Effect is *very different* from the classical *(inverse)* Gertsenshtein-Effect. With the Li-Effect, a gravitational wave transfers energy to a separately generated electromagnetic (EM) wave in the presence of a static magnetic field. That EM wave has the same frequency as the GW and moves in the same direction. This is the "*synchro-resonance condition*," in which the EM and GW waves are synchronized (move in the same direction and have the same frequency) and is unlike the Gertsenshtein- Effect.

The result of the intersection of the parallel and superimposed EM and GW beams, according to the Li-Effect, is *new EM photons moving off in a direction perpendicular to the beams and the magnetic field directions*. Thus, these new photons occupy a separate region of space (see Figure 12) that can be made essentially noise-free and the synchro-resonance EM beam itself (in this case a Gaussian beam) is not sensed there, so it does not interfere with detection of the photons. This Li-Effect was utilized by Baker (2001) in the design of the Li-Baker HFGW detector and Chinese Patent (Baker, 2000) of a device to detect HFGWs, the innovative Li-Baker HFGW Detector.

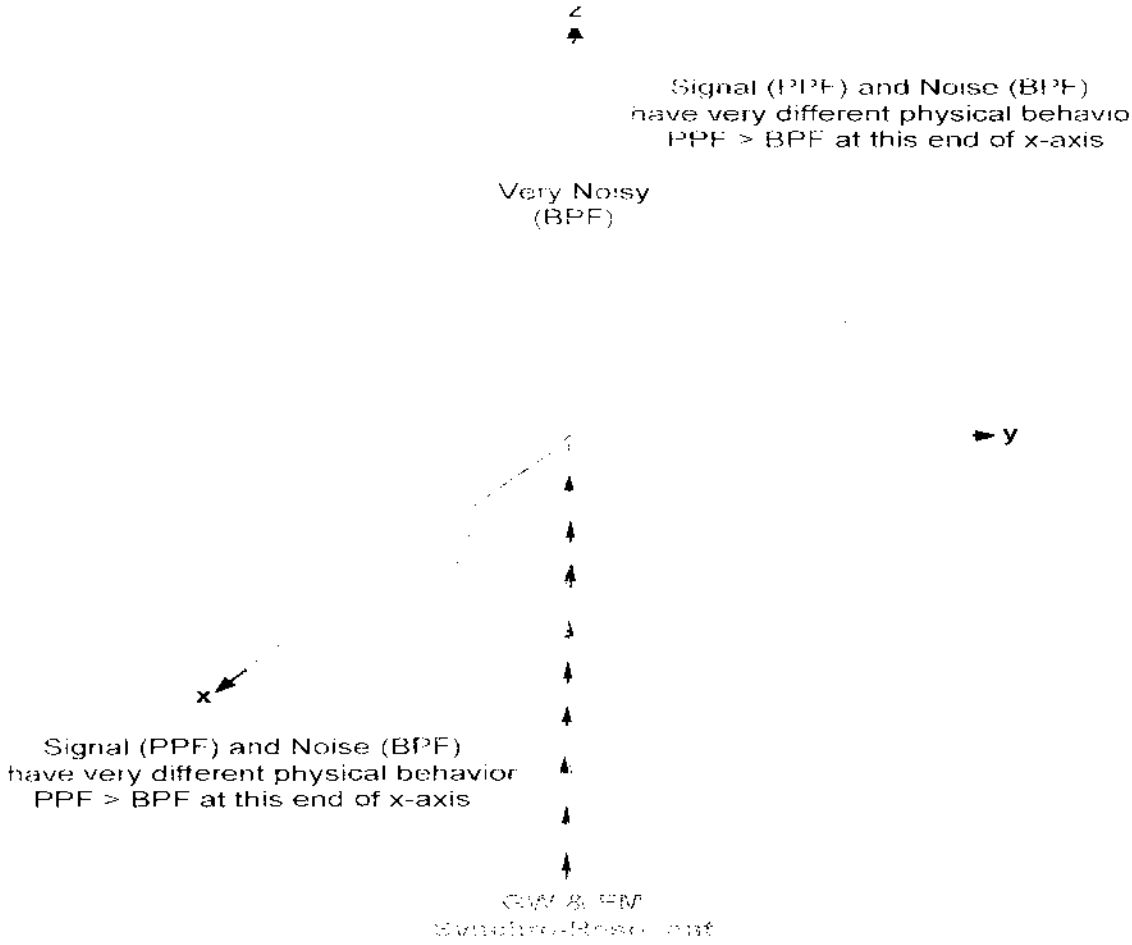

Figure 12. Detection Photons Sent to Locations That are Less Affected by Noise

The synchro-resonance solution of Einstein's field equations [Li *et al.* (2008), pp. 411 to 413] is radically different from the Gertsenshtein (1962) effect. The newer Li-Effect solution utilizes a coupling between EM and gravitational waves (Li, Tang and Zhao, 1992) that arises according to the theory of relativity. And a strong static magnetic field in the *y*-direction, *B*, is superimposed upon a GW propagating in the *z*-direction, as in the inverse Gertsenshtein effect. However, with the Li-Effect, there is an *additional* focused microwave beam ("Gaussian beam") at the expected frequency, phase and bandwidth of the HFGWs in the same direction (*z*) as the GW (as shown in Figure 12).

Unlike the Gertsenshtein effect, a *first-order* perturbative photon flux (PPF), comprising the detection photons, will be generated in the *x*-direction. Since there is a 90 degree shift in direction, there is little crosstalk between the PPF and the superimposed EM wave (Gaussian beam), so the PPF signal can be isolated and distinguished from the effects of the Gaussian beam, enabling detection of the GW.

Here's how it works:

The perturbative photon flux (PPF), which signals the detection of a passing gravitational wave (GW), is generated when the two waves (EM and GW) have the

same frequency, direction and phase. This situation is termed "synchro-resonance." These PPF detection photons a are generated as the EM wave propagates along its *z*-axis path, which is also the path of the GWs, as shown in Figure 12.

The magnetic field is in the y-direction. According to the Li-Effect, the PPF detection photon flux (also called the "Poynting Vector") moves out along the x-axis in both directions.

The signal (the PPF) and the noise, or background photon flux (BPF) from the Gaussian beam have very different physical behaviors. The BPF (background noise photons) are from the synchro-resonant EM Gaussian beam and move in the z-direction, whereas the PPF (signal photons) move out in the x-direction along the x-axis.

The PPF signal can be intercepted by electromagnetic-interference-shielded microwave receivers located on the *x*-axis (isolated from the synchro-resonance Gaussian EM field, which is along the *z*-axis). In addition, isolation is further improved by cooling the microwave receiver apparatus to greatly reduce thermal noise background (Baker, Stephenson and Li, 2008a).

The resultant efficiency of detection of HFGWs is very much greater than from the inverse Gertsenshtein effect, which has been exploited in some previously proposed HFGW detectors and found to have insufficient sensitivity to HFGWs (Eardley, et al., 2008). The amplitude of the PPF has space accumulation dependence—that is, it is proportional to the length of the wave overlap. This is because the GWs (gravitons) and EM waves (photons) have identical propagation velocities, so that the two waves overlap synchronously and coherently throughout and their interaction is cumulative (Boccaletti *et al.*, 1970; DeLogi and Mickelson, 1977). This is the synchro-resonant condition or Li-effect. This means that for maximum signal, the interaction overlap coupling must be as long as possible. It should be noted that the identification of this coupling or Li-effect, upon which the Li-Baker HFGW detector is based, is not so new that it is untested in the literature. At least nine peer-reviewed research publications concerning the theory have appeared following Li, Tang and Zhao (1992), including those by Li and Tang (1997), Li *et al.* (2000), Li, Tang and Shi (2003), Li and Yang (2004), Li and Li (2006), Li and Baker (2007), Li, Baker and Fang (2007), Baker, Stephenson and Li (2008a), and Li *et al.* (2008).

2.2.3 Quantum Back-Action Limit

The Standard Quantum Limit (SQL) will be introduced and reviewed in this section (Stephenson, 2009b), and design of the Li-Baker HFGW Detection System will also be reviewed to understand how the SQL might limit the sensitivity of this new type of GW detector.

Review of the Standard Quantum Limit

The Standard Quantum Limit (SQL) is often defined as "The limit on measurement accuracy at quantum scales due to back-action effects." But what is "back-action"? (See Kippenberg and Vahala, 2008.) From Clerk (2008) the Heisenberg Uncertainty Principle is

$$(\Delta x) \times (\Delta p) > \hbar/2 \qquad (3)$$

where Δx is the position uncertainty, Δp is the momentum uncertainty, and $\hbar$ is Planck's reduced constant. Thus measuring x disturbs p, which in turn disturbs future measurements of x

$$\Delta x(dt) = \Delta x(0) + dt[\Delta p(0)/m] \quad (4)$$

where $\Delta x(0)$ is the initial position uncertainty is, $\Delta p(0)$ is the initial momentum uncertainty, dt is the time of the future measurement, and m is the mass of the system under measurement. E/c^2 may be substituted for mass in an energy only system. This is depicted in Figure 13.

To summarize, the quantum effects of measurements on future measurements is quantum back action. Therefore the Standard Quantum Limit defines the lower sensitivity limit for all measurement instruments, including gravitational-wave detectors, according to the Heisenberg uncertainty principle. Detectors cannot avoid quantum back action, however the use of higher energies in the detection process can change the relative scale and impact of back action, and the use of squeezed states can shift the relative distribution of back action into states not involved in measurement.

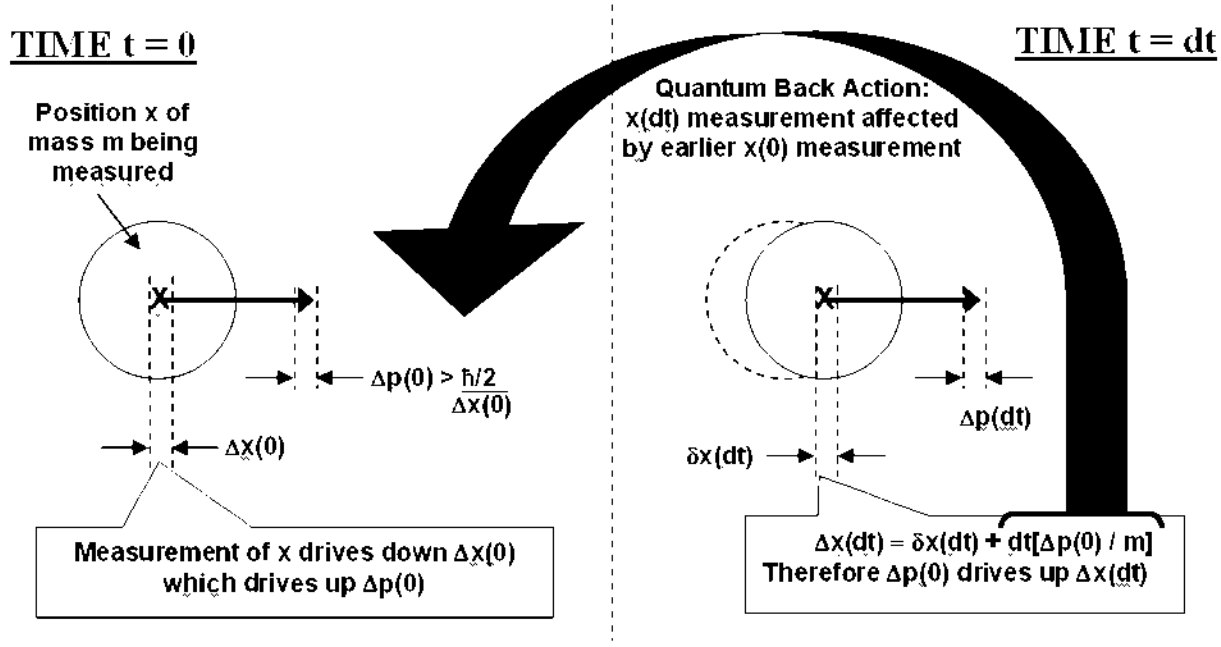

Figure 13. Quantum Back Action as a Mechanism for Creating the Standard Quantum Limit

Calculating the Standard Quantum Limit (SQL)

A method for calculating the Standard Quantum Limit (SQL) is introduced in this section. The calculation of coherent versus stochastic SQL is compared and contrasted. Important terms of the SQL calculation are described, including the impact of contained energy levels within the detector on SQL, and the sources of Quality Factor and its effect on SQL. Calculating the Standard Quantum Limit (SQL)

Coherent Versus Stochastic SQL

The question under consideration in this paper is whether or not the Li-Baker detector, Figure 14, is quantum-limited when detecting relic HFGW. In other words, does the standard quantum limit (SQL) interfere with the sensitivity of the Li-Baker detector design? The answer will be negative if the SQL is less than 10^{-32} m/m. Grishchuk (1977, 2007) has calculated the SQL for GW detectors in general, which for a coherent GW is

$$h_{det} = (1/Q)(\hbar\omega/E)^{1/2} \quad (5)$$

and for a stochastic GW is:

$$h_{det} = (1/Q)^{1/2}(\hbar\omega/E)^{1/2}, \quad (6)$$

where h_{det} is the metric (strain) detection limit in m/m, ω is the frequency of sensed gravitational waves (typically around 10 GHz in the Li-Baker detector), E is the effective energy contained within the detector cavity summed over the detection averaging time, and Q is the quality factor or selectivity of the signal over noise.

The SQL depends on the values of these parameters. For the remainder of this paper, we will consider the SQL of only the stochastic signal detection case. In the following subsections the best possible value of the SQL using current technology will be estimated to determine the fundamental limitations of the Li-Baker detector as now envisioned.

Impact of Contained Energy Levels on SQL

First attempt to estimate a realistic best case for the energy contained within the detection process, E. Typically it is expected that for a refrigerated microwave resonant cavity the best possible electrical quality factor will be around $2\pi\times10^5$. Assuming a "best efforts" value of 1000 W for the power of the Gaussian beam in a laboratory installation, the effective total RF energy stored in the microwave resonant cavity of the Li-Baker detector, summed over the system averaging time, is estimated to be given by (Grishchuk, 2007):

$$E_{RF} = (10^3 \text{ W}) \times (1000\text{s}) \times (2\pi\times10^5/2\pi) = 10^{11}\text{J} \quad (7)$$

over a typical 1000 s averaging time. Both the Li-Baker detector and a detector using the Gertsenshtein effect use a large static magnetic field B. For the present suggested outline design for the Li-Baker detector, the nominal value of B = 3 T, so that the magnetic energy density is given by

$$E_B = (\tfrac{1}{2})B^2/(\mu_r\mu_o) = 3.6\times10^6 \text{ Jm}^{-3} \cdot \quad (8)$$

The interaction volume in a practical laboratory-based detector is likely to be a maximum of around 1 m^3. So, the effective total stored energy from the Gaussian

beam is much greater than the stored magnetic field energy, and it follows that $E \approx E_{RF} = 10^{11}$ J to a reasonable approximation.

Sources of Quality Factor and Effect on SQL

To calculate the SQL, h_{det}, we also need the value of the detector quality factor Q (not the same as the cavity quality factor). Anything that concentrates or enhances the signal preferentially over noise, in any measurement dimension, can be considered a contributor to the quality factor Q. The quality factor can therefore be understood as the "signal selectivity" in each dimension, so that

$$Q_{tot} = (Q_{spatial})(Q_t) = Q_r Q_{solid\ angle} Q_t \ . \qquad (9)$$

The temporal quality factor in the Li-Baker detector arises from averaging the signal over time, so that at 10 GHz, $Q_t = \Omega t_{int} = (10\times10^9\ \text{Hz}) \times 1000\text{s} = 10^{13}$.

There is a contribution to Q arising from the fractal membranes that focus and concentrate the signal photon energy – but not the background photons – along the radial dimension. The radial selectivity arising from the general relativity solution, in conjunction with fractal membranes, is calculated by Li *et al.* (2008). Their table III gives $Q_r = SNR_{(r=37cm)}/SNR_{(r=3.5cm)} = 3.4\times10^{21}$.

This is mostly due to the effective Q contribution arising from the synchro-resonance solution to the Einstein field equations that limit the PPF signal to a radiation pattern in certain directions, whereas noise is distributed uniformly. By utilizing directional antennas, the Li-Baker detector can capitalize upon this gain due to the focusing power of fractal membranes as a contribution to Q in angular space as well. This is calculated in detail, octant by octant, by Li *et al.* (2008). Page 24 of Li *et al.* summarizes this in terms of angular concentration onto the detector. A non-directional antenna corresponds roughly to solid angle 2π steradians (one hemisphere), so that the effective antenna gain is estimated as $(Q_{solid\ angle}) = 2\pi\ \text{sr}/10^{-4}\text{sr} = 6.3\times10^4$. Therefore, the predicted maximum quality factor will be $Q_{total} = Q_r Q_{solid\ angle} Q_t = 2.1\times10^{39}$. This finally gives the Standard Quantum Limit (SQL) for stochastic GW detection at 10 GHz:

$$h_{det} = (1/Q)^{1/2}(\hbar\omega/E)^{1/2} = 1.8\times10^{-37}\ \text{m/m} \ . \qquad (10)$$

Comparison of SQL With Predicted Sensitivity

As noted in the previous section, $h_{det} = 1.8\times10^{-37}$ m/m represents the lowest possible GW amplitude detectable by each RF receiver in the Li-Baker HFGW detector, limited by quantum back-action. An additional $(1/\sqrt{2})$ factor applies if the separate outputs from the two RF receivers are averaged, rather than used independently for false alarm reduction, resulting in a minimum $h_{det} = 1.2\times10^{-37}$. Since the predicted best sensitivity of the Li-Baker detector in its currently proposed configuration is $A = 10^{-32}$ m/m, these results confirm that the Li-Baker Detector is photon-signal limited, not quantum noise limited; that is, the Standard Quantum Limit is so low that a properly designed Li-Baker detector can have sufficient sensitivity to observe HFRGW of amplitude $A \approx 10^{-32}$ m/m.

2.2.4 Li-Baker HFGW Detector

The detector, shown in Figure 14, has five major components:

1. A Gaussian (focused, with minimal side lobes) microwave beam (GB) is aimed along the +z-axis at the same frequency as the intended HFGW signal to be detected (Yariv, 1975), typically in the GHz band, and also aligned in the same direction as the HFGW to be detected. The microwave transmitter's horn antenna is not shown, but would be located on the –z-axis.

2. A static magnetic field B, generated by two powerful magnets, typically using powerful superconductor magnets such as those found in a conventional MRI medical body scanner, is directed along the *y*-axis.

3. Two paraboloid-shaped reflectors, which are formed from "fractal membranes" (Wen *et al.*, 2002; Zhou *et al.*, 2003; Hou *et al.*, 2005), are located in the y-z plane at the origin of the coordinate system to aim and focus the detection photons at diffraction-limited spot antennas connected to two microwave receivers. These reflectors, shown in planer form in Figure 15, are segmented (similar to a Fresnel lens) and located back-to-back in the y-z plane. They are thin enough (less than a centimeter thick in the x-direction) to not block the z-directed Gaussian beam. These microwave reflectors reflect the x-directed detection photons (PPF) and reject the z-directed Gaussian-beam photons, which move parallel to the surface of the reflectors in the y-z plane.

4. High-sensitivity shielded microwave receivers are located at each end of the x-axis each about one meter distant from the origin.

5. Interior noise from thermal photon generation is eliminated by cooling the Li-Baker detection apparatus to below ~ 48 mK (0.048 Kelvin). Thus there are effectively no thermal photons at 10 GHz. Noise from the interior background photon flux (BPF) from the EM Gaussian beam is reduced to a negligible level by moving the receivers out to the side about a meter away from the EM beam and by a series of superconductor or microwave absorbent baffles to "shade" the receivers. Stray EM resulting from scattering of particulate matter near the apparatus and possible dielectric dissipation can be effectively suppressed by evacuating the apparatus to about 7.5×10^{-7} Torr (a rather high vacuum). External noise is eliminated by the use of a steel and titanium cryogenic containment vessel surrounding the low-temperature Li-Baker detection apparatus.

In summary, several different HFGW receivers can be utilized for communication; but the proposed Li-Baker detector (plans & specification development in Appendix B) shows the most promise (detailed underlying concept is derived in the paper included as Appendix C).

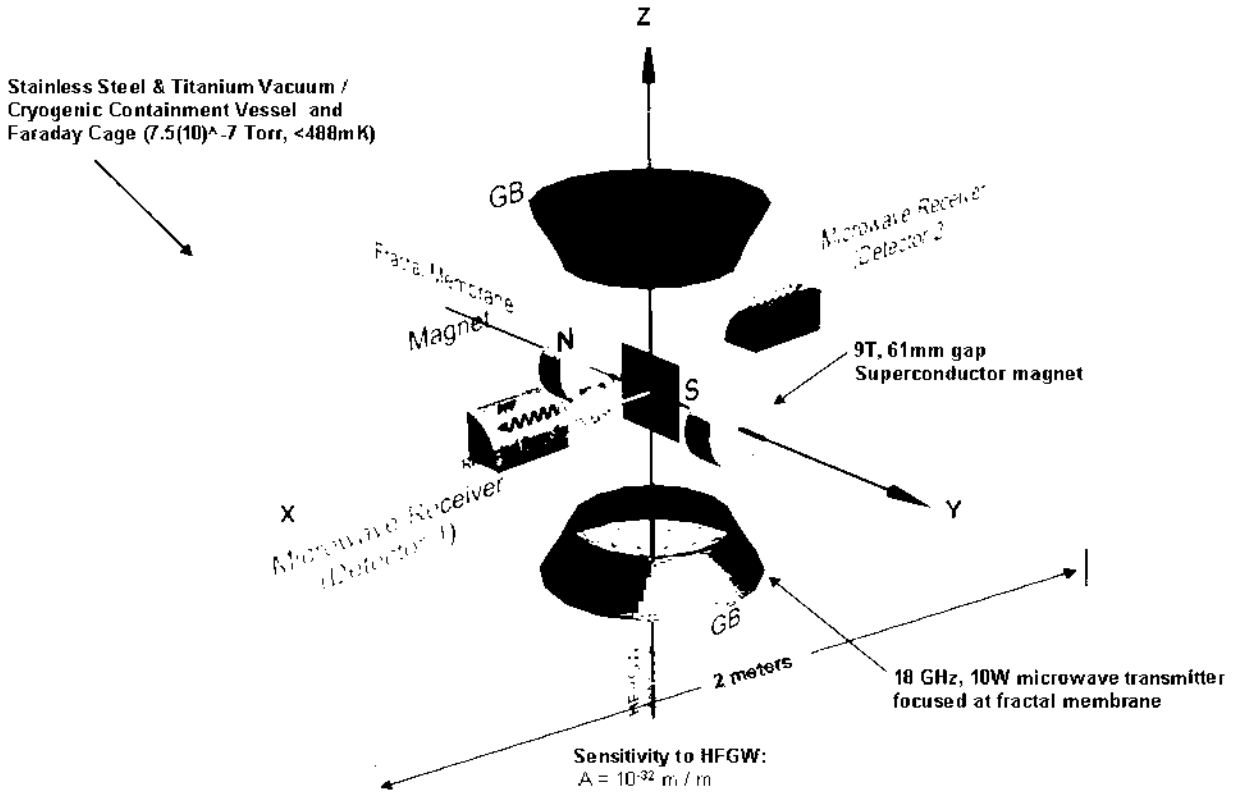

Figure 14. Schematic of Ultra-Sensitive HFGW Detector

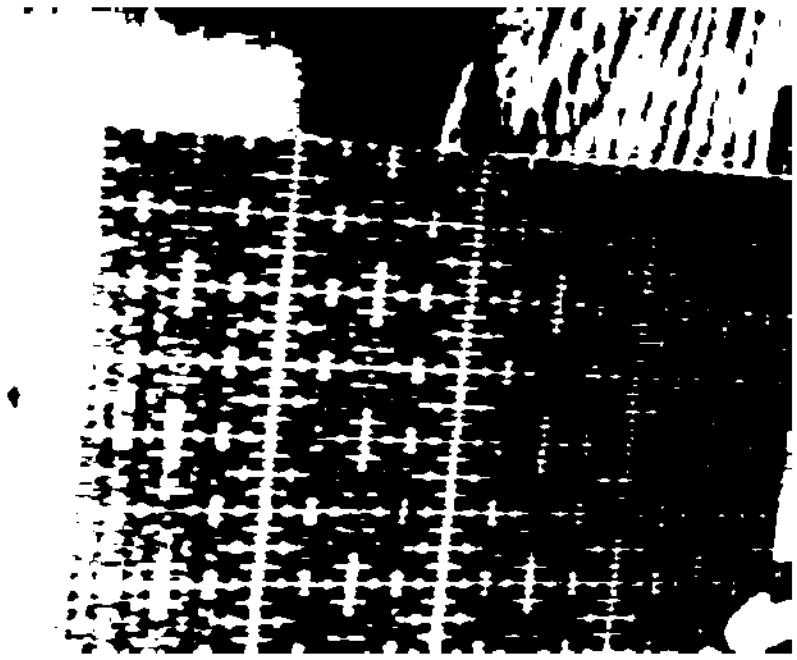

Figure 15. Fractal Membrane Component of Li-Baker Detector Exhibited in Planar Form

3.0 Operational Concerns

3.1 LINK BUDGET

3.1.1 Signal-to-Noise Ratio

Signal-to-noise ratio (SNR) is an important figure of merit in communication systems because it is an indicator of whether or not a transmitted signal will be useful upon arrive at its destination, the receiver. Without processing gain an SNR > 1 will be required to maintain a link budget. On the transmitter's end, the signal to noise is determined by the useful signal that is produced by the transmitter after it is already in its transmission mode, such as the GW power at the output of the GW generator antenna, divided by the RSS (Root Sum Square) of the uncorrelated noise sources referred to the same spot in the signal chain—that is, output referred noise equivalent power (NEP). This signal to noise ratio is represented by the left hand column in Figure 16.

The components of the transmitter's noise equivalent power may be sorted by the source of the noise. First, before the signal is converted to GW it is in the realm of EM or photon radiation. Photons themselves make noise, and this component goes as the square root of the total number of photons. Then there is thermal noise—that is, the photons generated by blackbody radiation of the transmitter components themselves. Other electronic and semiconductor components providing the source signal generate their own photon noise due to carrier activity. All these noise sources are carried along with the original EM signal and may be converted just as faithfully as if they were signals should they fall within the transmission bandwidth. All of this is just for the EM noise component.

The generation process itself may also be a source of noise, and will vary widely depending upon the generator method used. For example, the generation process noise created in the GASER would be significantly different than that created in a tuned resonant EM toroid cavity. This of course would be an important consideration in selecting a generator type.

Finally, it is expected that there are a variety of GW noise sources. Background sources from space are predicted, in low levels, across the entire frequency spectrum. Also, in a GW generator situation, parasitic vibrations may also have quadrupole moments, such as the walls of a generation cavity for instance, or an unwanted vibration within a slab of SC, and these could also generate GW noise.

Then there is link loss to contend with. While it is expected that the attenuation of GW due to absorption and scatter will be quite low, geometry alone will dictate that a spherically uniform radiating source will fall off as $1/R^2$. This link loss will affect both the transmitted signal and the transmitted noise.

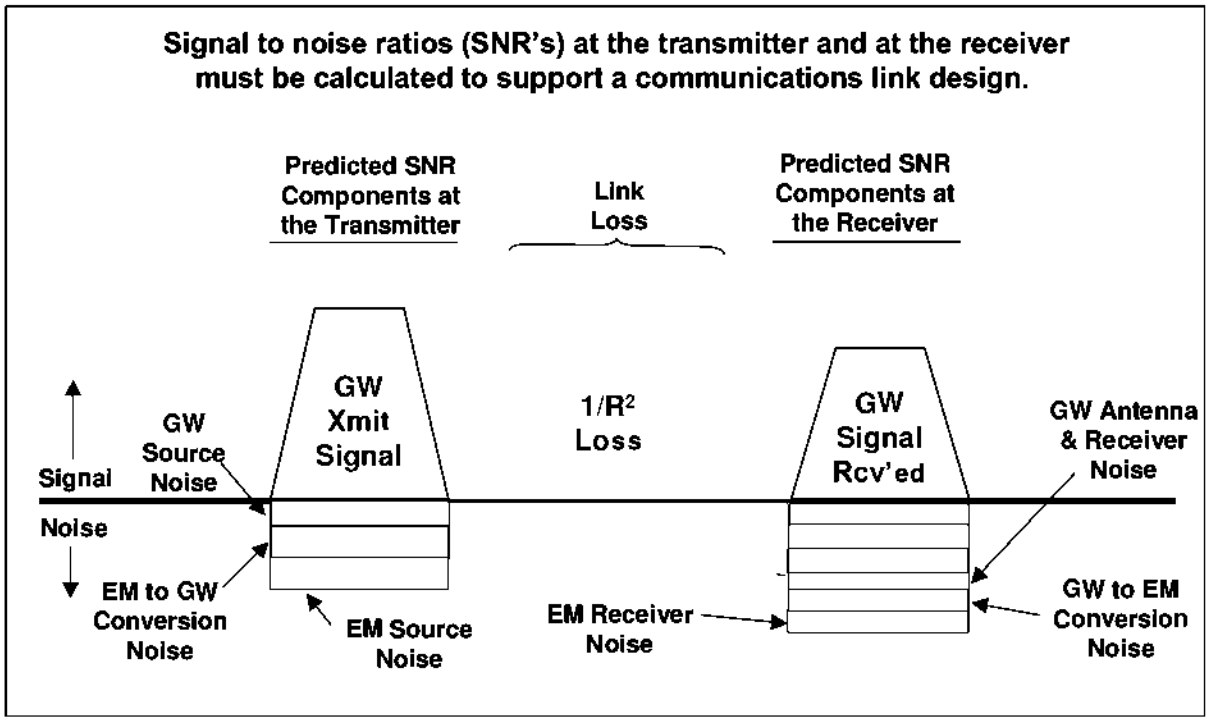

Figure 16. Conceptual SNR Fill Factors: Signal and Noise Components

In the receiver all these same noise sources are duplicated in reverse, as shown on the right had side of Figure 16. Referring power now to the input, there will be a received power, and the created by the receiver that was not created at the transmitter, also GW to EM conversion noise, and EM receiver noise of the same types as received propagated transmit noise. Added to this will be GW noise admitted or outlined for transmitters. When all these noise components are referred the input of the receiver, the total NEP, which is the RSS of all the noise components, must be less than the signal present at the input of the receiver to qualify as a useful link.

A few comments are in order regarding the "Q-factor" of the receiver. One way to increase Q is to narrow bandwidth. However, this has limited value. At some point, shrinking the bandwidth will shrink the signal received as quickly as the noise received, and some receiver noise components remain constant, resulting in a net drop in SNR. Another way to increase Q is to arbitrary increase sample times of the signal. This technique will, relatively speaking, shrink receiver end noise components as referred to the input of the receiver, but it will not have any impact of the noise generated at the transmitter. Therefore in this case the SNR will approach a constant. However, both of these approaches for improving sensitivity will have an adverse effect on the information capacity of the channel, which is important for a communication application.

3.1.2 Link Budget Considerations

Now consider the signal side of the communication challenge. The central question is, How do we close the link? That is, how much signal is necessary at the input of a communication channel to have a useful signal at the other end? These questions may be answered, qualitatively in this case, by considering the terms of the expression in

Figure 17. In general, an EM signal Si will be used to actuate some type of GW generation device, and this device will have a conversion efficiency of μ_{eg}, which represents the ratio of power of the EM input signal to power of the GW signal generated. Not all of the GW generated will be constructively used to radiate in the desired direction; some of the GW power will be lost to destructive interference, and some will not be radiated through the antenna aperture. Thus the transmitter will have a less than unity radiated power efficiency, R_x.

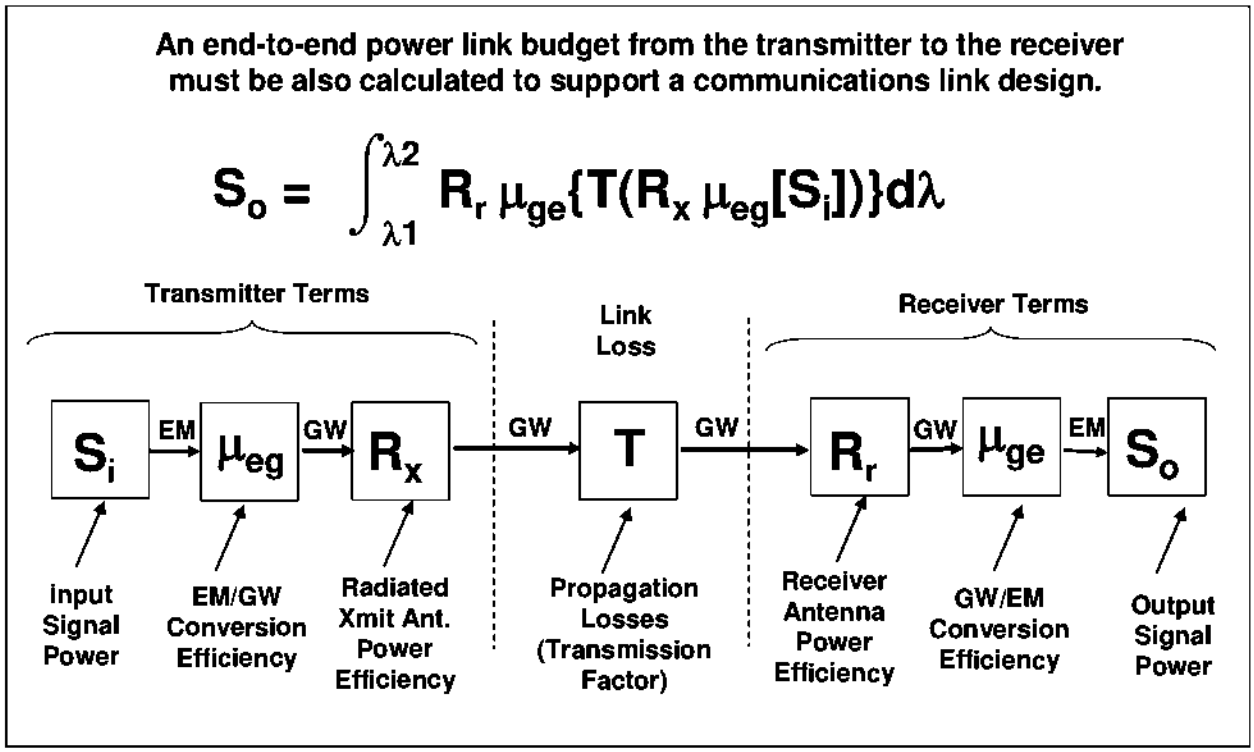

Figure 17. A Block Diagram of a Typical Link Budget

Then there will be propagation link loss, or transmission loss, T, which will be the antenna pattern integrated across the solid angle of the receiver antenna aperture as seen from the source. The receiver may have an GW antenna that aids in focusing an otherwise wider solid angle into a narrower detection aperture, and if this is true, then there will be an efficiency associated with this receiver antenna, designated here as R_r.

At the receiver's detector, there is another conversion factor to account for, the conversion efficiency of GW signal power to EM signal power μ_{ge}, which would be much less than unity, except that the Q factor enters the equation as a component of μ_{ge}. Of course Q may also impact the bandwidth range over which the signal is collected, L1 to L2. There is also a hidden integral here which occurs over the sample time, which is understood.

All of these terms will have to be defined and well understood before a communication system can be successfully designed. Many of these parameters have been predicted for the components reviewed in prior sections, however, they will not be verified until a successful experiment can be performed.

3.2 BANDWIDTH

An estimate of the bandwidth that a HFGW transglobal communication system might achieve, after a proof-of-concept test is successfully completed, based on a technical paper by Black and Baker (2009), is as follows: for a 50,000Å infrared (IR), 12.5 meter long,10-meter radius (10^4 concentric rings per plate so P_i = 1.29×10^2 Wm^{-2} and 10^7 plates) cylindrical HFGW generator (Woods and Baker, 2009), the flux at a one-meter distance from the generator is, according to Table 1 for $N = 10^7$, $(1.146\times10^{12}) \times (1.29\times10^2) = 1.48\times10^{14}$ Wm^{-2} (very large, and with a very narrow 2.3×10^{-4} radian half-power point needle beam). The required generator power can be reduced by utilizing pulsed HFGWs. Suppose that the distance between the generating or transmitting device and the detecting or receiving device is a little more than an Earth's equatorial radius, or ~ 7×10^6 meters. At this distance, 7000 km, the flux of the received signal, S, is $(1.48\times10^{14})/(7\times10^6)^2 = 3$ Wm^{-2}, more than adequate for an effective communication system.

With this configuration, the width of the needle-like, narrow HFGW beam at the receive end is $(2.3\times10^{-4}) \times (7\times10^6) = 1.6$ km, and multiple HFGW carrier frequencies can be used, so the signal is very difficult to intercept, and is therefore useful as a low-probability-of-intercept (LPI) signal, even with widespread adoption of the technology. From Equation (2), derived in the Appendix of Baker, Stephenson and Li (2008a), the amplitude A of the HFGW at 7,000 km with the HFGW frequency (twice the IR frequency of $v_{GW} = 1.2\times10^{14}$ s^{-1}) given by: $A = 1.28\times10^{-18}$ $S^{½}/v_{GW} = 1.8\times10^{-32}$ (in dimensionless units or m/m), which would be detectable by the currently designed Li-Baker HFGW detector. Since the exact frequency and phase of the HFGW signal is known (unlike big-bang relic HFGWs, for which the detector was designed), a much more sensitive, optimized HFGW detector will likely be developed.

Grishchuk (2008) indicates that there will be negligible relic HFGW noise at the IR HFGW generator's frequency of 1.2×10^{14} s^{-1} and no other cosmic sources at these frequencies are currently hypothesized. Prior to the proof-of-concept test, we will assume a noise figure at the Li-Baker detector of 10^{-8} Wm^{-2}.

Using C.E. Shannon's classical equation (1948), the maximum rate of information transfer, C, is given by:

$$C = B\log_2(1+S/N) \quad (3A)$$

$$C = B\log_2(1+3.0/10^{-8}) \sim 1.9\times10^6 \text{ bps} \quad (3B)$$

The bandwidth, B, here is arbitrarily taken to be 100 kHz for a future advanced system. The necessity for large temporal Q factors, ($Q_t \sim 10^9$), currently precludes bandwidths larger than a few Hz for early systems, but the use of coherent signals will represent an easing of sensitivity requirements significantly, improving bandwidth. Note that it is based on a single carrier chopping frequency, whereas in practice, one can spread the information over an entire band of HFGW frequencies.

3.3 FREQUENCY AND TIME STANDARD

The first application of HFGW to the distribution of frequency and time standard (FTS) data would be to assist otherwise conventional communications equipment. A typical near-Earth distribution system could conceivably result in a number and configuration

of the ground stations, shown in Figure 18 where their latitude and longitude are given in parentheses.

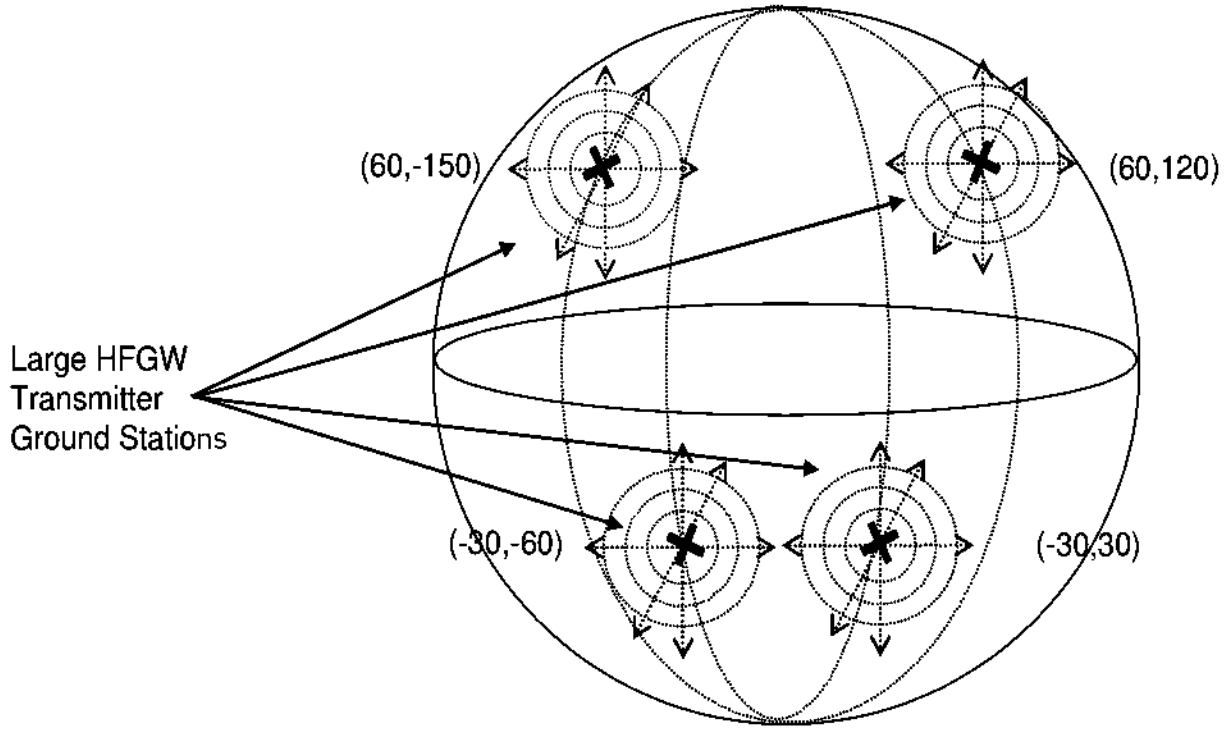

Figure 18. A Proposed Near-Earth Distribution of Frequency Time Standard

The large transmitter ground stations would provide the signals used as both the frequency and time standards. All FTS ground stations would be synchronized such that they emit signals exactly in phase with each other, all tied to a common frequency time source, such as the US Naval Observatory. Each station would use a different frequency such that the remote terminal (RT) user set could easily differentiate signals, and any phase or time difference observed would be due to either the relative position of the remote terminal with respect to each ground station, or the relative velocity of the remote terminal with respect to each ground station. Each ground station would transmit both a carrier wave (CW) signal for a frequency reference and a periodic pulse signal (PPS) for a time reference. At least 3 ground stations would be needed for self-triangulation by the remote terminals, at least 4 with redundancy. HFGWs will propagate through the Earth with little modification, but very slight HFGW phase modification may be observed in surveillance applications (Baker, 2007.)

The counterpart to the fixed ground infrastructure would be the remote terminal side or user side of the FTS infrastructure. Each remote terminal would need to be equipped with a small HFGW receiver, which could pickup all 3 or 4 ground stations simultaneously. The arrival times of the received PPS signals could be compared via time difference of arrival, or TDOA, and used to develop a position estimate. The CW signal phases could be compared to determine the Doppler velocity of the remote terminal with respect to an Earth Centered Inertial (ECI) coordinate system. Thus, the HFGW FTS system could be used as a navigational aid, akin to the GPS system. This end of the infrastructure would be receive only and could therefore be a very low power

device. Therefore mobile devices, such as portable remote spaceborne terminals could be typical users of such a navigational service. An example is depicted in Figure 19.

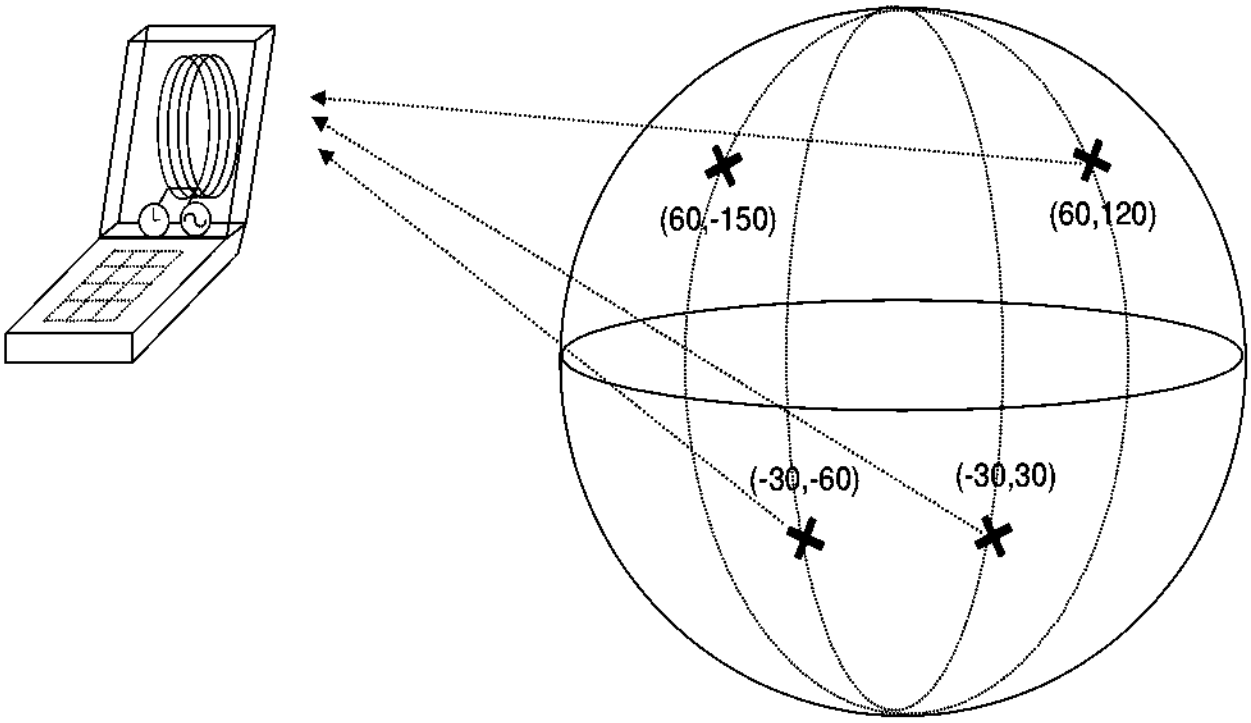

Figure 19. HFGW Supplemented Remote Terminal Design

The navigational sensitivity of the HFGW receiver would depend on the frequencies used in the HFGW FTS system, as the received CW HFGW signal would act as the remote terminal's "built-in" frequency standard, replacing the need for internal crystal oscillators or Cesium or Rubidium standards. An HFGW FTS carrier wave with a frequency of 300 GHz with a wavelength of 1 mm would result in 3 pico-second type time accuracy. The use of TDOA with these accuracies would allow for arbitrarily small navigational errors.

3.3.1 Improvements Accruing from a HFGW Time Standard

The cost of the FTS infrastructure must be more than balanced by the benefit resulting from that infrastructure if the cost is to be justified. Given that the GPS already provides adequate navigation services for most applications, navigational benefits alone would not justify the cost of an HFGW FTS system. However, in the case of a universal HFGW FTS, there are additional benefits associated with applying the frequency and time standards to standard telecommunications problems. The universal nature of the HFGW frequency and time standards are especially helpful. The following telecommunication benefits of an HFGW FTS system will be described in this section: improvement in acquisition time from search space improvements, improvements in modulation and coding efficiency from phase noise improvements, and improvements in bandwidth efficiency from frequency noise improvements.

3.3.2 Search Space Improvement Accruing From HFGW FTS

The following points are relevant with respect to the universal use of HFGW FTS among all remote terminals (including for instance cell phone handsets and their associated cellular towers):

- During signal acquisition the receiving terminal must perform a search of the search space of frequency, phase, and code to acquire the transmitting terminal signal.
- If there is less noise in these parameters the search space is reduced, speeding acquisition.
- Ultra-fast acquisition allows more efficient TDMA, or Time Domain Multiple Access style operations, such as transmit on demand, that use bandwidth more efficiently.

The smaller resultant search space is depicted graphically in Figure 20.

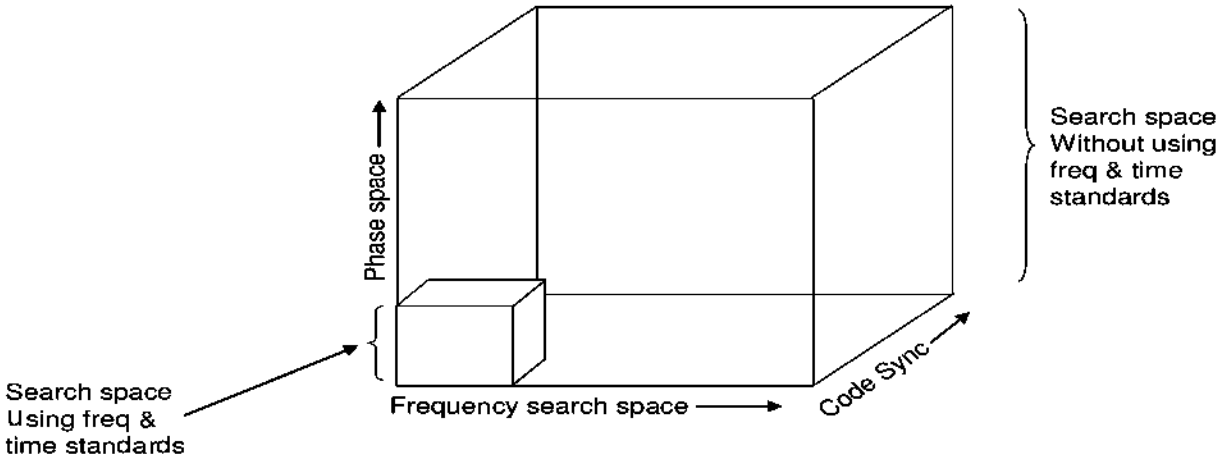

Figure 20. Acquisition Search Space Improvement Accruing from HFGW FTS

An equation for acquisition search space time is presented in Equation (12)

$$T_{acq} = N_{phase} * N_{freq} * N_{code} * (t_a) \quad (12)$$

where N_{phase} = number of phase space cases to check for acquisition,

N_{freq} = number of frequency cases to check for acquisition,

N_{code} = number of code sync possibilities to check and

t_a = acquisition test time, per test case.

In a typical example, if 30 MHz chipping is used with a 5 μsec error, there will be 150 code sync possibilities to check. If a case where a frequency error of 1 Hz is used within the acquisition window would cause a missed acquisition, and the worst case frequency error is 150 Hz, then the number of frequencies that must be checked is also 150. Finally, we must check each possible phase possibility, say 16 different options for 16-PSK. PSK stands for Phase Shift Keying and is the encoding of data bits using incremental phase modulation. These acronyms are specified in the nomenclature

section below. For a 5 μsec acquire test time, the result is T_{acq} = 150 × 150 × 16 × 5 μsec = 1.8 seconds acquisition time.

However, with effectively perfect knowledge of time, frequency, and hence also phase, there will only be one case to check, so result is T_{acq} = **1** × 1 × 1 × 5 μsec = 5 μsec acquisition time. This is essentially instantaneous for applications such as TCP/IP or VoIP. This will favorably impact the overall TDMA efficiency in that it speeds the claiming process to the point where an "always on" link can be replaced by a "link on demand." This is a savings of 25 to 50 percent in channel usage for VoIP and TCP/IP sessions over "always on."

3.3.3 The Impact of Phase Noise Improvements on Phase Shift Encoding

The use of a universal HFGW FTS would also benefit the relative phase noise of all terminals, allowing for finer phase encoding. Phase noise limits the type of modulation and manner of encoding that can be performed in phase space, commonly used for over the air telecommunication systems. An HFGW FTS system could reduce phase noise by providing a frequency reference with outstanding stability. For example, moving from QPSK to 8PSK or 16-PSK improves bandwidth efficiency by a factor of 2 to 4. The phase space improvement is summarized in Figure 21.

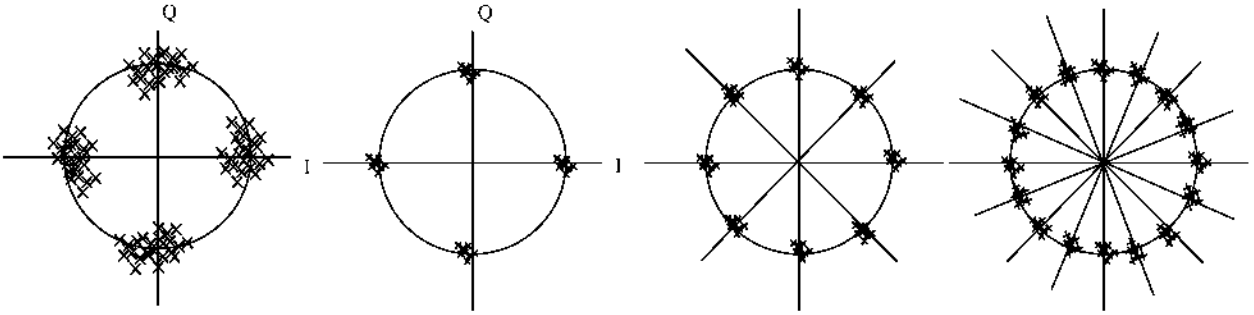

Figure 21. The Impact of Phase Noise Improvements on Phase Shift Encoding

In the example of Figure 21 nominal performance allows only QPSK, but improved phase noise would allow higher density phase encoding. Data rate will scale linearly with encoding efficiency as shown in Equation (13):

$$\text{Data Rate} = (BW/2) \times (\text{Coding Efficiency}) \times (\text{FEC Rate}) / (\text{PN Spreading Factor}) \quad (13)$$

Coding efficiency will be a factor of 2 better when moving from QPSK to 8PSK, or a factor of 4 better when moving from QPSK to 16-PSK. This will translate directly into a linear increase in the allowable data rate that a given bandwidth can support. Put another way, a universal frequency time standard could quadruple over the air bandwidth efficiencies just by improving phase noise alone. Phase noise improvements would be limited only by the slight variations induced in the HFGW signal passing through the earth as described in Baker (2007).

3.3.4 The Impact of Frequency Noise Improvements on FDMA and FHSS

The very low noise frequency standard that would be supplied by an HFGW FTS system would allow for much more efficient use of reserved frequency bandwidth. Frequency noise limits the type of modulation and manner of encoding that can be performed in frequency space, such as Frequency Division Multiple Access (FDMA) or Frequency Hopping Spread Spectrum (FHSS). HFGW can reduce frequency noise by providing a frequency reference with outstanding stability. For example, guard bands can be shrunk in FDMA, and frequency slices can be smaller and more stable in FHSS.

A frequency space representation of the FDMA and FHSS noise improvements are depicted in Figure 22.

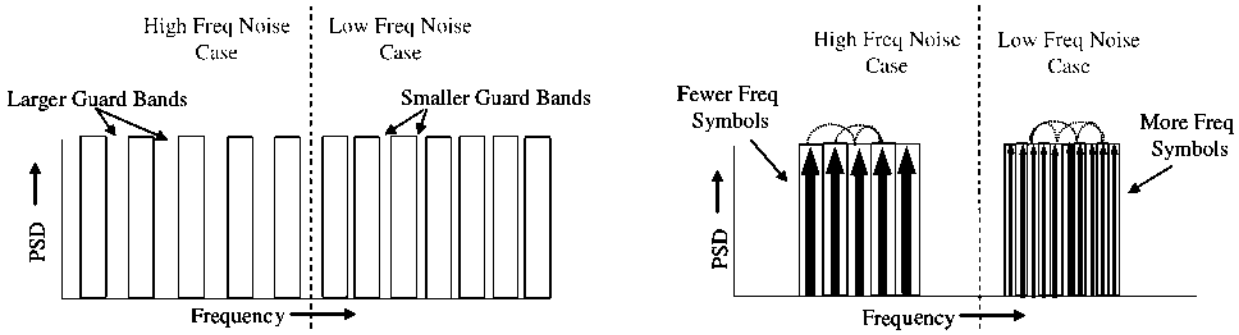

(**a**) Frequency Division Multiple Access. (**b**) Frequency Hop Spread Spectrum.

Figure 22. The Impact of Frequency Noise Improvements on FDMA and FHSS

Efficiencies in guard-band structure can be defined as in Equation (14).

Guard band BW Efficiency = (Total Bandwidth –{Sum of Guard BW})/Total Bandwidth (14)

Guard bands often consume 30 to 50 percent of assigned frequency space. While guard bands would still be required to allow for the side lobes of signals, the frequency error component would be eliminated. Similar efficiencies may be gained in the FHSS approach. A better knowledge of absolute frequency allows better frequency coding efficiencies, as seen in Equation (13) and depicted in Figure 21.

3.4 POSSIBLE FUTURE UPGRADES TO THE FTS DEVICES

Per the 9 Feb 2009 issue of *New Scientist*, optical lattice clocks are under development that will lead to a dramatic improvement over the current standard Cesium atomic oscillation clocks that now provide frequency time standard references. Optical lattice clocks vibrate at optical frequencies rather than microwave frequencies, with the reference frequency mixed down via frequency combs to allow measurements back down in the microwave regime. Strontium lattice clock are already operating with measurement precisions of 1 part in 10^{16}, and theoretical performance approaches 1 part in 10^{18}. At this precision one could measure the time delay caused by changing once centimeter in height in the Earth's gravitational field.

3.4.1 Propagating Signals From Optical Lattice Clocks for Timing

The 1 part in 10^{18} measurement precision of optical lattice clocks will be affected by general relativity effects, in other words propagation delays due to gravitational field gradients will be readily measureable. "It will make us think a little harder about what we really mean by time," Kleppner (2008). In effect, measuring the propagation delays at this level allows very fine measurement of the "geoids," or surfaces of constant gravity, surrounding planets and inhabiting interplanetary and interstellar space. The delay experienced by RF waves could therefore be precisely compared with the propagation delay experienced by gravitational waves, which are not as strongly affected by the presence of mass. Such a differential propagation delay comparison (between RF & GW) could lead to an important new technology in the mapping of geoids, which could for instance be applied to the problem of mapping the positions of the Lagrangian points, which vary slightly over time.

3.4.2 In Navigating and Mapping Interplanetary Geoids

The importance of locating and navigating to Lagrangian points is well established (Baker, 1967). See Figure 23 for a depiction of the Earth's Lagrangian points and their uses.

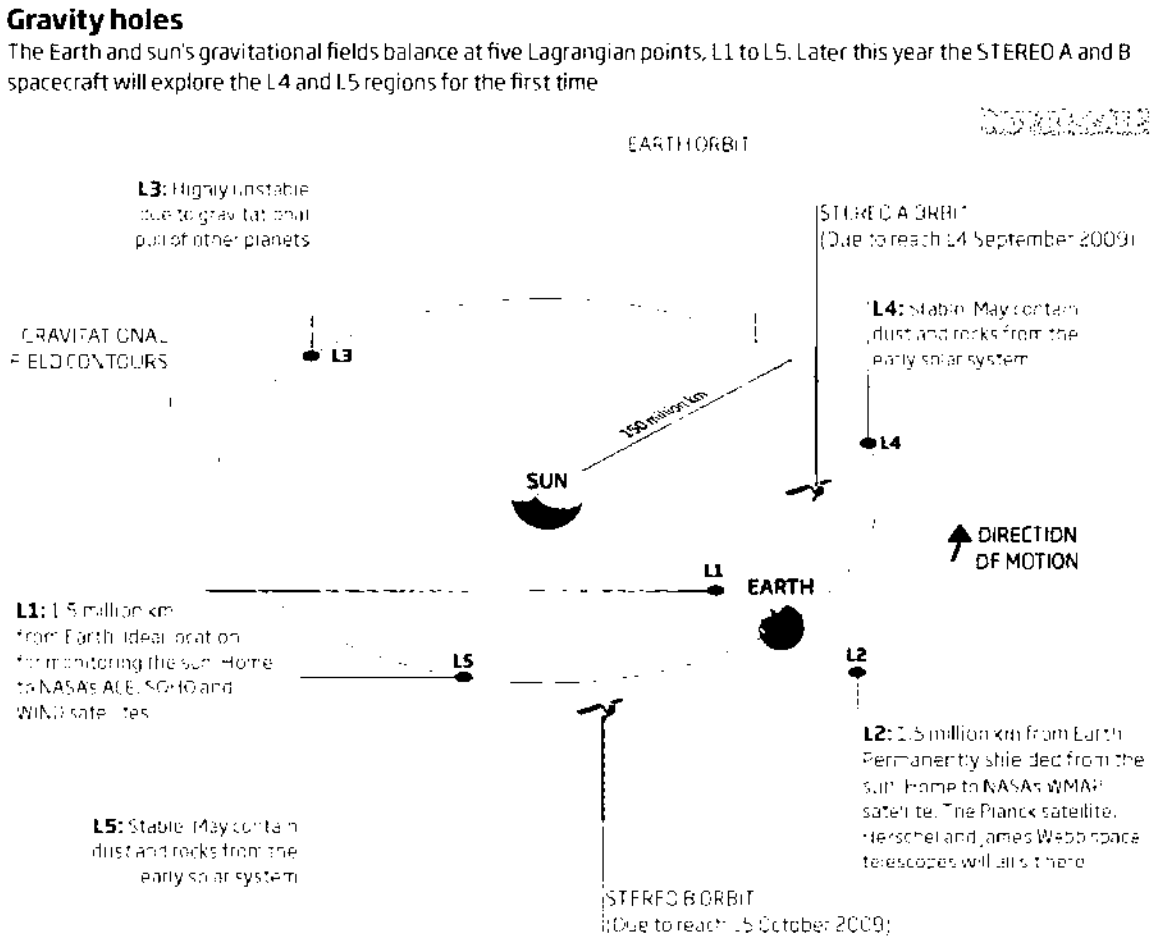

Figure 23. The Earth's Associated Lagrangian Points [New Scientist, 9Feb09 and Baker (1967), p.128, Figure 2.2]

L1 is an ideal location for solar monitoring, whereas **L2** is permanently shielded from the sun.

4.0 Future Potential

4.1 DEVELOPMENTAL ROADMAP

A development roadmap is suggested here for the application of High Frequency Gravitational Waves (HFGWs) in the field of communications. The development roadmap should be twofold:

- Theoretical work should continue on HFGW transmitters (generators) and receivers (detectors).
- Experimental devices should be built and tested in the laboratory and then transitioned over to a practical communications system.

A suggested developmental roadmap schedule and phasing timeline is included as Figure 24. Theoretical research is always an ongoing enterprise, but it is especially important to encourage work in the development of experimental approaches aimed at demonstrating laboratory generation and sensing of gravitational waves for the next few years. This is the kind of academic work that is best done in a research university setting, at least for the next ten years or so, until laboratory experiments can verify laboratory generation. Without early confirmation the technology will not gain widespread acceptance and move forward.

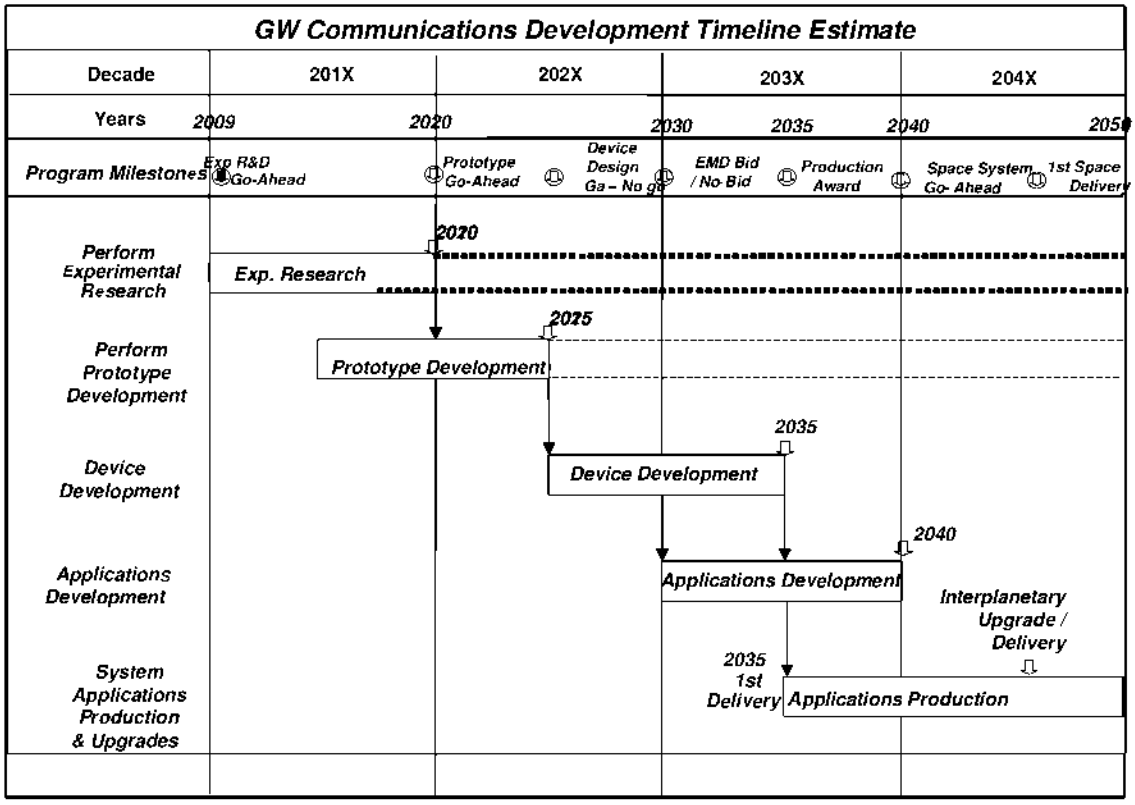

Figure 24. HFGW Com Space Application Development Roadmap, Estimated Timeline

The most benefit would come from a coordinated effort spread over a number of different universities. Wherever possible, pre-existing assets should be utilized to stretch funding as far as possible. For example, if synchrotron light is needed to verify the Gertsenshtein effect and the Li-effect, a survey of existing national synchrotron light facilities should be part of the funded effort to find an appropriate host facility. The funding activity—that is, the National Science Foundation—would have the overall responsibility to coordinate this activity in an ongoing manner, through proposal review, contract awards, and progress reviews, and the approach should be flexible enough to allow the redirection of funding should a particularly promising new technology or invention move to the forefront.

Assuming that positive laboratory results can be achieved and peer reviewed in a 10 to 12 year timeframe, the next step would call for a period of prototype development, in which the device physics and engineering needed to support the technology could be matured. As prototypes show promise they could be transitioned to device development, the first time that industry would likely enter the field. Once the individual devices required to support GW communication technology—for example, GW generators and GW sensors—are in place, at that point it will be possible to begin full-scale development of systems applications. This is a conservative timeline, based on scaling from the development of previous technologies. If breakthroughs materialize, or if the pace of technological development quickens, progress may certainly occur more quickly than this.

4.2 HFGW COMMUNICATIONS PREDICTIONS TO 2050

In what follows, with an eye to the future, extrapolations are made concerning the development of a HFGW communications technology into the far future (for example, 2050 and beyond). It is difficult to predict even ten years in advance to the time when we expect to have the results of the proof-of-concept test (or "Bell-Watson" experiment) are available and the immediate applications to HFGW communications completed. Speculation beyond that time will be contingent upon advanced development of FBAR crystals, new materials within the toroidal waveguides, and so forth, or even entirely new approaches such as those proposed by G. Fontana, V. Rudenko, R. Chiao, et al. No doubt the Li-Baker detector performance can also be greatly improved with stronger magnetic fields, more intense Gaussian beams, and better baffles as well as new detector designs yet to be developed possibly based upon theories developed at Birmingham University, INFN Genoa and The National Astronomical Observatory of Japan. Optimum designs of communication channels, bands and modulation are also be anticipated. Many of these advanced concepts were discussed at the 3rd HFGW Workshop in Huntsville in February 2009. Nanotechnology advances will allow for the fabrication of smaller and smaller HFGW transceivers having millimeter dimensions and milliwatt power requirements by 2050 and "Radio ID" or rather "HFGW ID" nanochip tags may be ubiquitous. Gravitational wave transmissions would also have the advantage of being able to pierce the protective plasma shielding that may in the future be routinely used to protect the crew aboard manned vessels—that is, communications through artificial magnetospherics, a technological limit of RF communications.

4.3 INTERPLANETARY NAVIGATION AND GEOID MAPPING TO 2050

While there is no doubt that stellar tracking will remain the primary source of navigation for space missions in the foreseeable future, as introduced in Section 3.4.2, HFGW may also prove useful in conjunction with RF in providing a navigation aid for interplanetary missions (with no planetary shielding) by mapping geoids in interplanetary space via long baseline navigation. For instance, if there were one GW source on Earth, and one GW source on the Moon, such a pair of GW sources would provide relative beacons for missions to Mars that could serve multiple roles as navigation beacons, communication relays, and in conjunction with RF signals, map geoids via relative time difference of arrival signals. Very Long Baseline Navigation could be achieved by placing a source on Earth and one GW source on Mars for a baseline that would most often be very widely spread with respect to the outer planets, for outer planetary missions. See Figures 25-27 for a number of different navigation beacon pair options.

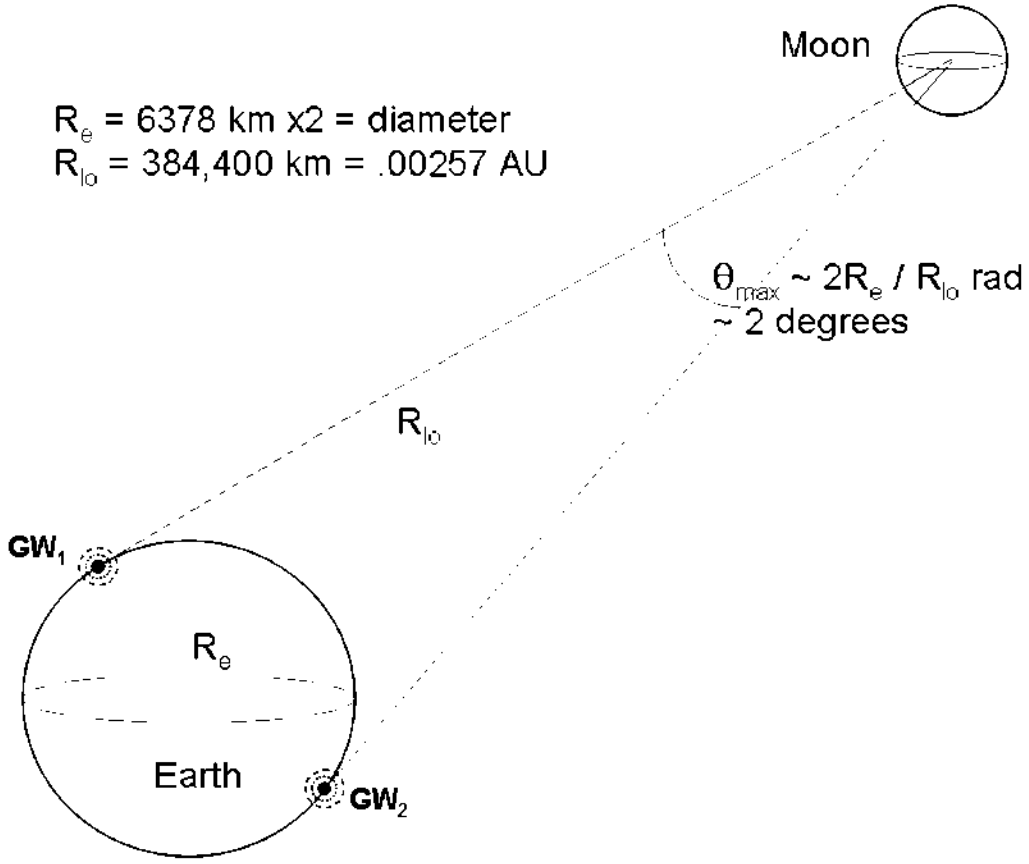

Figure 25. A GW Pair on Earth as Used by a Lunar Mission

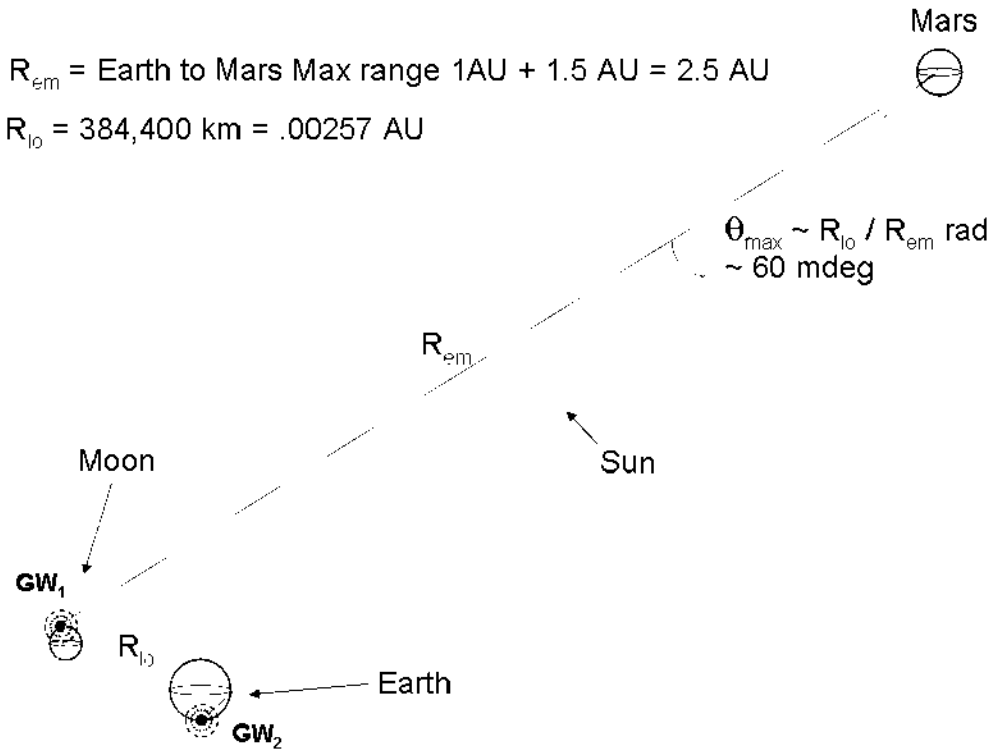

Figure 26. A GW Pair on Earth and on the Moon, as Used by a Mission to Mars

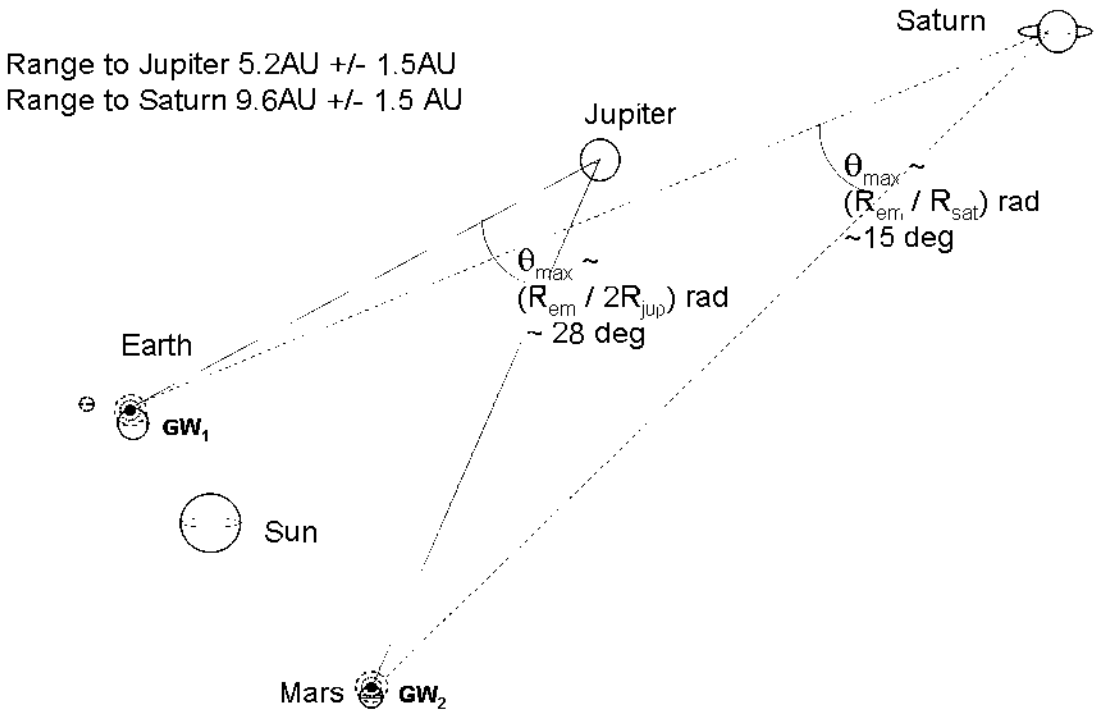

Figure 27. A GW Pair on Earth and on Mars for an Outer Planetary Reference Pair

4.4 OTHER POSSIBLE HFGW APPLICATIONS

The most stunning advances in HFGW applications will probably not be in communications, but in the remotely HFGW-generated nuclear fusion, HFGW propulsion and HFGW surveillance. If an ultra-high-intensity HFGW flux impinges on a nucleus, it is possible that it could initiate nuclear fusion at a remote location, or mass disruption. Also it may be possible to create radioactive waste-free nuclear reactions and energy reactions (Fontana, G. and Baker, R. M L, Jr. 2007). As they suggest: "At high amplitudes, GR (Gravitational Radiation) is nonlinear, thus we might expect a departure from geometric optics. Fortunately, the problem has been already theoretically examined and the resulting effects are found to be advantageous. Nonlinearity improves the focusing process and h goes to one in finite time, producing a singularity "regardless" of the starting, non-focused amplitude of the impinging gravitational wave (Corkill and Stewart, 1983; Ferrari, 1988a; Ferrari 1988b; Ferrari, Pendenza and Veneziano, 1988; Veneziano, 1987; Szekeres, 1992). The effect of a $\Delta h = 0.995$ pulse of HFGWs on the couple formed by a deuterium nucleus and its electron is the reduction of their relative distance by a factor of 200. If this distance reduction is effective for a few picoseconds, then the two nuclei of a deuterium molecule can fuse and give an He atom plus energy, which is the usual nuclear-fusion process in a star."

HFGWs could theoretically be used for propulsion and control of the motion of objects such as missiles, missile warheads, spacecraft, and asteroids, and remote control of clouds of hazardous vapors. Gravitational field changes by one or more HFGW generators could urge a spacecraft in a given direction, causing a lower static gravitational field in front of a vehicle (it "falls" forward) and a higher one behind (providing a "push"). The concept is that the mass essentially "rolls" down a "hill" produced by the static g-field; that is, potential energy increase of a mass is provided by the energetic HFGWs. The magnitude of the static g-field is proportional to the square of the HFGW frequency (Landau and Lifshitz, 1975, section 108, page 349). Specifically:

"Since it has definite energy, the gravitational wave is itself is the source of some additional gravitational field (static g-field). Like the energy producing it, this field is a second-order effect in the h_{ik}. <u>But in the case of high-frequency gravitational waves the effect is significantly strengthened</u>: the fact that the pseudotensor t^{ik} is quadratic in the derivatives of the h_{ik} introduces the large factor λ^{-2}. In such a case we may say that the wave itself produces the background field (static g-field) on which it propagates. This [static g] field is conveniently treated by carrying out the averaging described above over regions of four-space with dimensions large compared to λ. Such an averaging smooths out the short-wave "ripple" and leaves the slowly varying background metric (static g-field)." (Brackets and underline added for clarity and emphasis.)

Such an application must also await the future development of very high-intensity HFGW generators.

A novel means of imaging or HFGW surveillance might be developed in future to establish a system to allow for observing activities and materials in three dimensions, within and below structures and within the Earth and its oceans. Gravitational waves, including HFGWs, pass through most material with little or no attenuation; but although they are not absorbed, their polarization (Li and Nan, 2009), phase velocity (causing

refraction or bending of gravitational rays), backscatter, and/or other characteristics can be modified by a material object's texture and internal structure. For example, the change in polarization of a GW passing through a material object is discussed in Misner, Thorne, and Wheeler (1973): "In the real universe there are spacetime curvatures due not only to the energy of gravitational waves, but also more importantly to the material [objects and structures] content of the universe ... its wavelength changes [based on gravitational red shift] and [the gravitational wave] backscatters off the curvature to some extent. If the wave is a pulse, then the backscatter will cause its shape and polarization...." It is difficult to theoretically establish the actual magnitude of the changes, especially at very high frequencies (10^{14} Hz and higher) and to quantify them prior to HFGW generation/detection laboratory experiments.

4.5 2050 AND BEYOND

The phases of human space exploration may be divided into the following phases:

- Epoch 1 – Interplanetary Exploration
- Epoch 2 – Interstellar Exploration
- Epoch 3 – Intergalactic Exploration
- Epoch 4 – Universal Exploration

Each phase will have its own challenges and opportunities, but one can certainly speculate that the human need for connectedness and communication knows no bounds. So any scope of expansion beyond Epoch 1 will have enormous challenges in the area of communication. The vast distances involved will require some form of communication that entails faster-than-light (FTL) propagation. While this is a highly speculative area, such schemes have been proposed for FTL HFGW. Both Fontana and Meholic (unpublished reports) have proposed models of the universe, such as the trispace model, in which subluminal or luminal gravitational waves may couple into a super-luminal "parallel universe" inside which FTL speeds are possible. Such as scheme would be required to communicate between star systems and galaxies if humankind is to maintain any type of cohesive civilization. Without communications we have a history of fractured civilization, and we slip into becoming our own worst enemy. Universal communication holds the lofty promise of universal peace.

5.0 Acknowledgements

The research published in technical papers authored by Gary Stephenson, chief investigator for Seculine Consulting, (Stephenson, 2009a, Harper Stephenson (2007) and Stephenson (2009b)) were crucial in the preparation of this study and is gratefully acknowledged.

6.0 References

Baker, R. M L, Jr. (1967), *ASTRODYNAMICS: Applications and Advanced Topics*, Academic Press, New York and London

Baker, R. M L , Jr. (2000), Chinese Patent Number 0510055882.2

Baker, R. M L, Jr. (2001), U. S. Patent Number 6,784,591

Baker, R. M L, Jr. (2006), "Novel formulation of the quadrupole equation for potential stellar gravitational-wave power estimation," *Astronomische Nachrichten* **327**, No. 7, pp. 710-713.

Baker, R. M L, Jr., Woods, R. C. and Fangyu Li (2006), "Piezoelectric-Crystal-Resonator High-Frequency Gravitational Wave Generation and Synchro-Resonance Detection," *Space Technology and Applications International Forum (STAIF-2006)*, edited by M. S. El-Genk, American Institute of Physics Conference Proceedings Vol. **813**, Melville NY, pp. 1280-1289.

Baker, R. M L, Jr., Stephenson, G. V. and Li, F. (2008a), "Proposed Ultra-High Sensitivity HFGW Detector," *Space Technology and Applications International Forum (STAIF-2008)*, edited by M. S. El-Genk, American Institute of Physics Conference Proceedings Vol. **969**, Melville, NY, pp. 1045-1054.

Baker, R. M L, Jr., Stephenson, G. V. and Li, F. (2008b), "Analyses of the Frequency and Intensity of Laboratory Generated HFGWs," *Space Technology and Applications International Forum (STAIF-2008)*, edited by M. S. El-Genk, American Institute of Physics Conference Proceedings Vol. **969**, Melville, NY, pp. 1036-1044.

Bernard, P. Gemme, G., Parodi, R. and Picasso, E. (2001), "A detector of small harmonic displacement based on two coupled microwave cavities," *Review of Scientific Instruments* **72,** Number 5, May, pp. 2428-2437.

Black, C. S. and Baker, R. M L, Jr. (2009), "Radiation Pattern for a Multiple-Element HFGW Generator," *Space, Propulsion and Energy Sciences International Forum (SPESIF)*, 24-27 February, ed. G. Robertson, 3rd High-Frequency Gravitational Wave Workshop (Paper 035), American Institute of Physics Conference Proceedings, Melville, NY, in press.

Boccalet D., Desabbar V., Fortini P. and Gualdi C. (1970), "Conversion of Photons Into Gravitons and Vice Versa in a Static Electromagnetic Field," Il Nuovo Cimento **B70,** 129

Braginsky, V. B. Grishchuk, L. P., Doroshkevich, A.G., Zeldovich, Ya. B. Noviko, I. D. and Sazhin, M. V. (1974), "Electromagnetic Detectors of Gravitational Waves," *Sov. Phys. JETP* **38**, p. 865.

Braginsky, V. B. and Rudenko, Valentin N. (1978), "Gravitational waves and the detection of gravitational radiation," Section 7: "Generation of gravitational waves in the laboratory," *Physics Report* (Review section of *Physics Letters*) **46**, Number 5, pp. 165-200.

Chapline, G. Nuckolls, F. J. and Woods, L. L. (1974), "Gravitational-radiation production using nuclear explosions," *Physical Review D.* **10,** Number 4, August, pp. 1064-1065.\

Chiao, R. Y. (2007), "New Direction for gravity-wave physics via 'Millikan oil drops,'" 6 April, arXiv:gr-qc/0610146v6.

Chiao, R. Y., Minter, S. J., and Wegter-McNelly, K. (2009a), "Do Mirrors for Gravitational Waves Exist?," arXiv:0903.0661v5 [gr-qc], March 23.

Chiao, R. Y., Minter, S. J., and Wegter-McNelly, K., (2009b), "Laboratory-scale superconducting mirrors for gravitational microwaves," arXiv:0903.3280v3 [gr-qc], March 26.

Chincarini, A and Gemme, G. (2003), "Micro-wave based High-Frequency Gravitational Wave detector," paper HFGW-03-103, *Gravitational-Wave Conference,* The MITR Corporation, May 6-9.

Cruise, A. M. (2000), "An electromagnetic detector for very-high-frequency gravitational waves," *Class. Quantum Gravity* **17**, pp. 2525-2530.

Cruise, A. M. and Ingley, R. M. J. (2005), "A correlation detector for very high frequency gravitational waves," *Class. Quantum Grav.* **22**, 5479-5481.

Cruise, A. M. (2008), "Very High Frequency Gravitational Waves," Gravitational Wave Advanced Detector Workshop (GWADW), Elba Conference, 17 May, slide presentation 132.
https://indico.pi.infn.it/contributionDisplay.py?contribId=132&sessionId=13&confId=225

Clerk, A.A. (2008), "Quantum Noise & Quantum Measurement," (APS Tutorial on Quantum Measurement),"McGillUniversity website, http://www.physics.mcgill.ca/~clerk/PDFfiles/APSQMeasTutorialMar08.pdf.

Dehnen, H. and Fernando Romero-Borja (2003), "Generation of GHz – THz High-Frequency Gravitational Waves in the laboratory," paper HFGW-03-102, *Gravitational-Wave Conference,* The MITRE Corporation, May 6-9.

DeLogi W.K. and Mickelson A.R. (1977), "Electro-Gravitational Conversion Cross-Sections in Static Electromagnetic-Fields," *Phys. Rev.* **D16,** pp. 2915-2927

Douglass, D.H. and Braginsky, B. (1979), "Gravitational-radiation experiments," in "General relativity: an Einstein centenary survey" Ed. Hawking S.W. and Israel W. (CUP, UK), 90-137.

Eardley, et al. (2008) "High Frequency Gravitational Waves," JSR-08-506, October, the JASON defense science advisory panel and prepared for the Office of the Director of National Intelligence.

Einstein, Albert (1915), Einstein, Albert (1915), "Die Feldgleichungen der Gravitation," Sitzungsberichte der Preussischen Akademie der Wissenschaften zu Berlin: 844–847, http://nausikaa2.mpiwg-berlin.mpg.de/cgi-bin/toc/toc.x.cgi?dir=6E3MAXK4&step=thumb, retrieved on 12 September 2006 (General Relativity)

Einstein, Albert (1916), Einstein, Albert (1916), "Die Grundlage der allgemeinen Relativitätstheorie" (PDF), Annalen der Physik 49, http://www.alberteinstein.info/gallery/gtext3.html, retrieved on 3 September 2006 (Gravitational Waves)

Einstein, Albert, (1918) Über Gravitationswellen. In: Sitzungsberichte der Königlich Preussischen Akademie der Wissenschaften, Berlin (1918), 154–167. (Quadrupole equation and formalism)

Fontana, G. (1998), "A possibility of emission of high frequency gravitational radiation from junctions between d-wave and s-wave superconductors," Preprint, Faculty of Science, University of Trento, 38050 Povo (TN), Italy, pp. 1-8. http://xxx.lanl.gov/html/cond-mat/9812070.

Fontana, G. and Baker, R. M L Jr. (2003), "The high-temperature superconductor (HTSC) gravitational laser (GASER)," paper HFGW-03-107, *Gravitational-Wave Conference,* The MITRE Corporation, May 6-9.

Fontana, G. and Baker, R. M L, Jr. (2006), "Generation of Gravitational Waves with Nuclear Reactions," *Space Technology and Applications International Forum (STAIF-2006)*, edited by M. S. El-Genk, American Institute of Physics Conference Proceedings Vol. **813**, Melville, NY, pp. 1352-1358.

Fontana, G. and Baker, R. M L Jr. (2007), "HFGW-Induced Nuclear Fusion," *Space Technology and Applications International Forum (STAIF-2007)*, edited by M. S. El-Genk, American Institute of Physics Conference Proceedings Vol. **880**, Melville, NY, pp. 1156-1164.

Fontana, G. and Binder, B. (2009), "Electromagnetic to Gravitational wave Conversion via Nuclear Holonomy," *Space, Propulsion and Energy Sciences International Forum (SPESIF)*, 24-27 February, ed. G. Robertson, Paper 015, American Institute of Physics Conference Proceedings, Melville, NY, in press.

Grishchuk, L. P. and Sazhin M. V. (1974), "Emission of gravitational waves by an electromagnetic cavity." *Soviet Physics JETP* **38**, Number 2, pp. 215-221.

Grishchuk, L. P. (1977), "Gravitational Waves in the Cosmos and the Laboratory," *Usp. Fiz. Nauk* **121**, pp 629-656.

Grishchuk, L. P. (2003), "Electromagnetic generators and detectors of gravitational waves," paper HFGW-03-119, *Gravitational-Wave Conference,* The MITRE Corporation, May 6-9.

Grishchuk, L.P. (2007) "High-Frequency Relic Gravitational Waves, their Detection and New Approaches," in the proceedings of the HFGW2 Workshop, Institute Austin (IASA), Texas, September 19-21; http://earthtech.org/hfgw2/, accessed 11/06/08.

Grishchuk, L.P. (2008), "Discovering Relic Gravitational Waves in Cosmic Microwave Background Radiation," Proceedings of the School, Eds. I. Ciufolini and R. Matzner, (in press) Springer 2008, arXiv:0707.3319v3

Halpren, L. and Laurent, B. (1964), "On the gravitational radiation of a microscopic system," *IL NUOVO CIMENTO*, Volume XXXIIIR, Number 3, pp. 728- 751.

Harper, C. and Stephenson, G.V. (2007), "The Value Estimation of an HFGW Frequency Time Standard for Telecommunications Network Optimization," *Space Technology and*

Applications International Forum (STAIF-2007), edited by M. S. El-Genk, American Institute of Physics Conference Proceedings Vol. **880**, Melville, NY, pp. 1083-1091.

Hou B., Xu G., Wong H.K., and Wen W.J. (2005), "Tuning of photonic bandgaps by a field-induced structural change of fractal metamaterials," *Optics Express* ***13*** 9149-9154.

Ingley, R. M. J. (2005), "Implementation and Cross Correlation of Two High Frequency Gravitational Wave Detectors," Ph.D. Thesis, *The University of Birmingham,* January.

Kippenberg, T. J. and Vahala, K. J. (2008), "Cavity Optomechanics: Back-Action at the Mesoscale," Science 321, 1172-1176, August 29

Kleppner, D. (2008) Ref link: http://www.newscientist.com/article/mg20126941.900-super-clocks-more-accurate-than-time-itself.html?full=true

Kolosnitsyn, N. I. and Rudenko, V. (2007), "Generation and Detection of the High Frequency Gravitational Radiation in a Strong Magnetic Field," in the proceedings of the HFGW2 Workshop, Institute of Advanced Studies at Austin (IASA), Texas, September 19-21; http://earthtech.org/hfgw2/

Kraus. J. D. (1991), "Will gravity-wave communication be possible?" *IEEE Antennas & Propagation Magazine,* Volume 33, Number 4, August.

Landau, L. D. and Lifshitz, E. M. (1975), *The Classical Theory of Fields*, Fourth Revised English Edition, Pergamon Press, pp. 348, 349, 355-357.

Li, F. Y., Tang M. and Zhao P. (1992), "Interaction Between Narrow Wave Beam-Type High Frequency Gravitational Radiation and Electromagnetic Fields," *Acta Physica Sinic*a **41** 1919-1928

Li, F. Y. and Tang M.X. (1997), "Positive definite problem of energy density and radiative energy flux for pulse cylindrical gravitational wave," *Acta Physica Sinica* **6** 321-333.

Li, F. Y., Meng-Xi Tang, Jun Luo, and Yi-Chuan Li (2000) "Electrodynamical response of a high energy photon flux to a gravitational wave," *Physical Review D* **62**, July 21, pp. 044018-1 to 044018 -9.

Li, F. Y., Meng-Xi Tang, and Dong-Ping Shi, (2003), "Electromagnetic response of a Gaussian beam to high-frequency relic gravitational waves in quintessential inflationary models," *Physical Review B***67**, pp. 104006-1 to -17.

Li, F. Y. and Nan Yang (2004), "Resonant Interaction between a Weak Gravitational Wave and a Microwave Beam in the Double Polarized States Through a Static Magnetic Field" *Journal-ref:Chin. Phys. Lett.* **21,** No. 11, p. 2113.

Li, F. Y. and Li, Ruxin (2006), "Ultra-High-Intensity Lasers for Gravitational Wave Generation and Detection," *Space Technology and Applications International Forum (STAIF-2006)*, edited by M. S. El-Genk, American Institute of Physics Conference Proceedings Vol. **813**, Melville, NY, pp. 1249-1258.

Li, F. Y. and Baker, R. M L, Jr. (2007), "Detection of High-Frequency Gravitational Waves by Superconductors," *6th International Conference on New Theories, Discoveries and Applications of Superconductors and Related Materials*, Sydney, Australia, January 10; *International Journal of Modern Physics* **21**, Nos. 18-19, pp. 3274-3278.

Li F.Y., Baker R. M L and Fang Z. (2007), "Coupling of an open cavity to a microwave beam: a possible new scheme for detecting high-frequency gravitational waves," after peer review accepted for the Proceedings of the AIP Space Technology and Applications Int. Forum, Albuquerque, New Mexico **880,** 1139-1147.

Li F. Y., Baker R. M L, Jr., Fang Z., Stephenson G.V. and Chen, Z. (2008), "Perturbative Photon Fluxes Generated by High-Frequency Gravitational Waves and Their Physical Effects," European Phys. J. C 22, Nos. 18-19, 30 July; available at http://www.drrobertbaker.com/docs/Li-Baker%20Chinese%20HFGW%20Detector.pdf http://www.gravwave.com/docs/Li-Baker%206-22-08.pdf (please see Appendix C).

Li, Fangyu and Yang Nan (2009), "Phase and Polarization State of High-Frequency Relic Gravitational Waves," *Journal of Chinese Physics Letters* (in press). Misner, C. W. Thorne, K. and Wheeler, J. A. (1973), *Gravitation*, W. H. Freeman and Company, New York.

Ottaway, D. J. et al (1998), "A Compact Injection-Locked Nd:YAG Laser for Gravitational Wave Detection," *IEE Journal of Quantum Electronic* **34,** Number 10, October 9.

Pegoraro, F., Radicati, L. A., Bernard, .Ph. and Picasso, E. (1978), *Phys. Rev. Letters A* **68**, p. 165.

Pinto, I. P. and Rotoli, G. (1988), "Laboratory generation of gravitational waves?" *Proceedings of the 8th Italian Conference on General Relativity and Gravitational Physics*, Cavlese (Trento), August 30 to September 3, World Scientific-Singapore, pp. 560-573.

Romero, F. B and Dehnen, H. (1981), "Generation of gravitational radiation in the laboratory," *Z. Naturforsch* **36a,** pp. 948-955.

Rudenko, V. N. and Sazhin, M. V. (1980), "Laser interferometer as a gravitational wave detector," *Sov. J. Quantum Electron* **10**, November, pp. 1366-1373.

Rudenko, V. N. (2003), "Optimization of parameters of a coupled generator-receiver for a gravitational Hertz experiment," paper HFGW-03-113, *Gravitational-Wave Conference,* The MITRE Corporation, May 6-9.

Shannon, C. B. (1948), *Bell Systems Technical Journal*, Volume **27**, Number 379, p. 623.

Shawhan, P. S. (2004), "Gravitational Waves and the Effort to Detect them," *American Scientist* **92**, 356. (Explains why LIGO cannot detect HFGWs.)

Stephenson, G. V. (2009a), "Lessons for Energy Resonance HFGW Detector Designs Learned from Mass Resonance and Interferometric LFGW Detection Schemes," *Space, Propulsion and Energy Sciences International Forum (SPESIF)*, 24-27 February, ed. G.

Robertson, Paper 016, American Institute of Physics Conference Proceedings, Melville, NY, in press.

Stephenson, G. V. (2009b) "The Standard Quantum Limit for the Li-Baker HFGW Detector," *Space, Propulsion and Energy Sciences International Forum (SPESIF)*, 24-27 February, ed. G. Robertson, Paper 023, American Institute of Physics Conference Proceedings, Melville, NY in press.

Tobar, M, ***1729-1736*** E. (1995), "Characterizing multi-mode resonant-mass gravitational wave detectors," *Journal of Applied Physics* **28,** pp. 1729-1736

Tobar, M. E. (1999), "Microwave Parametric Transducers for the Next Generation of Resonant-Mass Gravitational Wave Detectors," *Dept. of Physics, the University of Western Australia*, Nedlands, 6907 WA, Australia.

Weber, J. (1964), "Gravitational Waves" in *Gravitation and Relativity*, Chapter 5, pp. 90-105, W. A. Benjamin, Inc., New York.

Woods, R. C. and Baker, R. M L, Jr. (2005), "Gravitational Wave Generation and Detection Using Acoustic Resonators and Coupled Resonance Chambers," *Space Technology and Applications International Forum (STAIF-2005)*, edited by M. S. El-Genk, American Institute of Physics Conference Proceedings Vol. **746**, Melville, NY, p. 1298.

Woods, R. C. and Baker, R. M L, Jr., (2009) "Generalized Generators of Very-High-Frequency Gravitational Waves Including Ring and Helix Devices," *Space, Propulsion and Energy Sciences International Forum (SPESIF)*, 24-27 February, ed. G. Robertson, American Institute of Physics Conference Proceedings, Melville, NY, in press.

Yariv A. (1975), "Quantum electronics," 2nd Ed. (Wiley, New York), 1975

Yoon, K. W., Ade, P. A. R., Barkats, D., et al. (2006), "The Robinson Gravitational Wave Background Telescope (BICEP): a bolometric large angular scale CMB polarimeter," in Proceedings of the SPIE, **6275**: Millimeter and Submillimeter Detectors and Instrumentation for Astronomy III, ed. J. Zmuidzinas, W. S. Holland, S. Withington, and W. D. Duncan, Bellingham, Washington, astro-ph/0606278

Zhou L., Wen W., Chan C.T. and Sheng P. (2003), "Reflectivity of planar metallic fractal patterns," *Appl. Phys. Lett.* **82** 1012-1014.

Appendix A: Nomenclature

A	amplitude of gravitational wave, metric strain in spacetime, m/m
B	bandwidth, s^{-1}
B	magnetic field strength, Tesla
c	speed of light in vacuum (2.998×108 ms^{-1})
C	maximum rate of information transfer, bits per second (bps), s^{-1}
dt	time of future measurement, s
E	effective energy contained within the detector cavity summed over the detection averaging time, J
F_{GW}	gravitational-wave flux, Wm^{-2}
h	strain, m/m
h_{det}	(strain) detection limit, m/m
η	Planck's reduced constant 1.055×10^{34} Js
N	noise, Wm^{2}
N	number of linearly arranged GW radiation elements, integer
N_{phase}	number of phase space cases to check for acquisition, integer
N_{freq}	number of frequency cases to check for acquisition, integer
N_{code}	number of code sync possibilities to check, integer
n	number of pairs of oppositely jerking at one-time mass elements, integer
P	power of the generated gravitational waves, W
Q	temporal quality factor or selectivity of the signal-to-noise ratio, dimensionless
R	range, m
R_{cvr1}	receiver 1
R_{cvr2}	receiver 2
R_r	receiver antenna power efficiency, dimensionless
R_x.	radiated power efficiency, dimensionless
S	signal strength, Wm^{-2}
S_i	input signal strength, Wm^{-2}
S_o	output signal power, W
r	distance between two jerking-mass, gravitational-wave radiation elements, m
T	propagation or transmission-factor losses, dimensionless
t_a	acquisition test time per test case, s
t_{int}	integration or signal averaging time, s
X_{mit1}	transmitter 1
X_{mit2}	transmitter 2
Δf	change in force of a jerking-mass, gravitational-wave radiation element, N
Δp	momentum uncertainty, kg-ms^{1}
Δt	time interval, s
Δx	initial position uncertainty, m
μ_{eg}	conversion efficiency (ratio of power of the EM input signal to power of the GW signal generated), dimensionless
μ_{ge}	conversion efficiency (ratio of power of the GW input signal to power of the EM signal generated), dimensionless
λ	wavelength, m
v_{GW}	gravitational-wave frequency, s^{1}
ω	frequency of sensed gravitational waves, s^{-1}
ω_1	transmitting frequency, s^{-1}
ω_2	receiver-sensitivity frequency, s^{-1}

Appendix B: Li-Baker HFGW Detector

Appendix B describes a joint academia/industry project to design the ultra-high sensitivity Li-Baker detector for high-frequency gravitational waves (HFGWs). The partnership consists of Louisiana State University (LSU) and Transportation Sciences Corporation (TSC) in California. The Li-Baker HFGW detector exploits a solution of field equations that couples photons and GW in first order, and the sensitivity of the detector will be much better than previously-proposed HFGW detectors. The outcome of this study will be an engineering-ready design for the HFGW detection system, to be developed under continued funding. Future construction of this detector will broaden the search spectrum of the existing LIGO low frequency GW detection system; it will be used to detect and characterize the relic HFGW cosmological background radiation, contributing to clarifying the origins of the universe. This offers the first and best hope of GW detection in a completely new GW frequency régime around 10GHz, near the cutoff of what is cosmically generated and a proof of the capability of the detector to sense the HFGW emissions of the HFGW generator discussed in Sections 4.4, 4.5 and 4.6.

This first activity is to develop designs, plans and specifications for the Li-Baker configuration for ultra-high sensitivity detection of relic high-frequency gravitational waves (HFRGWs) in the laboratory. The first goal will be to develop the design to a stage where the likely performance can be evaluated in detail. Following a future proposal, the Li-Baker detector will subsequently be built and used for the basic-science purposes of sensing HFRGWs having their origin related to the "big bang," as well as for detecting laboratory-generated HFGWs (Romero and Dehnen, 1981; Baker, 1999, 2000; Woods and Baker, 2005, 2009). As discussed in Sections 4.4, 4.5 and 4.6 .Use will primarily be made of "off-the-shelf" components, and components described in the open scientific literature and in the various patents issued to Project Scientist **Robert M L Baker, Jr.** (Baker, 1999, 2000, 2001, and Patents Pending) who is the inventor of the Li-Baker HFGW Detector (Baker, 2001). Other components will be designed by the project participants during the Detector Design (DD) process. The project plan and timing are described below under separate headings for each component of the work.

DD1.1 Containment Vessel

Design of the cryogenic containment vessel and vacuum system: **Dr. R.C. Woods (LSU) + graduate student**, **G.V. Stephenson (TSC), Dr. R. M L Baker (TSC)**. This will be divided into four subtasks:

DD1.1.1 Selection of material for the containment vessel: this choice will be made in light of the vessel's approximate size and shape, initially anticipated to be cylindrical, overall approximately 2m diameter and 3m length. Manufacturing ultra-high vacuum chambers requires fabrication that ensures leak-free performance. For example, Meyer Tool & Manufacturing, Inc. (Oak Lawn, Illinois) supplies custom chambers for ultra-high vacuum (UHV) applications. Companies such as Meyer will be consulted and/or visited to evaluate their manufacturing capability. The final selection from the expected short-list of titanium, stainless steel and/or aluminum containment vessels will be made based upon manufacturer recommendation and evaluation of test data.

DD1.1.2 Detailed design of brackets and fixtures for the internal equipment, wiring, piping and through-wall connections: the general principles demonstrated by existing Magnetic Resonance Imaging (MRI) system designs (for example, from Siemens MRI, GE Healthcare, and others) will be followed to determine the most compatible design of the internal equipment, wiring, piping and through-wall connections for the HFGW detector. A cryostat or cryogenic containment vessel supported inside the vacuum vessel will house the superconducting magnet assembly necessary for the Li-Baker detector. Through-wall fittings and seals for copper leads supplying the magnet and other internal apparatus will be needed. Design of brackets, wiring, and piping of detector equipment will also be based upon input from the other tasks.

DD1.1.3 Design of vacuum system: there are a large number of "off-the shelf" Ultra-High Vacuum (UHV) equipment providers such as: Varian, Inc. (Lexington, Massachusetts), Kimball Physics, Inc. (Wilton, New Hampshire), and Edwards High Vacuum Ltd. (UK), amongst others. Those with capability for producing a system able to evacuate the chamber to about 10^{-7}Torr for the HFRGW detector will be approached to undertake a detailed specification.

DD1.1.4 Detailed design of size and shape of containment vessel: determination of the containment vessel's precise dimensions will be based upon the final designs of the equipment determined by the other tasks and will integrate all the specific sub-task designs, resolving any conflicts between units.

DD1.2 Signal Processing

Design of the recording apparatus hardware and software development that will be needed to handle merging the two receiver inputs over an averaging period of up to 1,000s: **Dr. R. M L Baker (TSC), G.V. Stephenson (TSC)**. This will require the conceptual design of digitizing hardware and software to handle the data gathered, including the combination of multiple receiver signals, the use of delay histograms, statistical filtering techniques, and the study of false alarm pitfalls in non-linear signal processing. There is much overlap with this area and DD1.5, the design of the detection receivers. The expected GW signal structure must be characterized to optimize the matched filtering needed. The definition of a detection event is the foremost consideration, and will be studied both in terms of the threshold level and in terms of the statistics of exceeding that level. Expected signal to noise enhancements ("processing gain") will be investigated for various filtering and processing options, and the effect of the *Q*-factor inherent in the detection apparatus will be included in this area of the investigation. Linear processing techniques such as multiple receiver combination and delay histogram searches will be studied, and nonlinear signal processing will also be considered, including its effect on detectability, as well as its effect on false alarm generation. This task includes the selection of the best computing and digitizing recorder platforms for the signal-processing needed. Also under this task is an investigation of whether magnetic field modulation can be used to advantage in this detector. Any scattered BPF does not depend upon the applied magnetic field or on the GW. Therefore, the wanted PPF can be "labeled" by varying the applied (nominally static) magnetic field in some way. A common technique in magnetic resonance experiments is to use field modulation coils that superimpose upon the constant applied magnetic field a time-varying component at low frequency (for example, around 50Hz but asynchronous with the commercial power supply frequency). As a result, the PPF is

"labeled" as whatever is recovered from the receivers at the same frequency as (and indeed phase-locked to) the modulation, so therefore the PPF can be distinguished from scattered BPF very easily. Typically a lock-in amplifier (referenced to the field modulation) is used to recover the signal in such an arrangement, which provides significant noise rejection by effectively reducing the detection bandwidth.

DD1.3 Microwave Transmitter (Gaussian beam)

Design of the microwave transmitter for the Gaussian beam, directed towards the central fractal membranes: **Dr. R.C. Woods (LSU) + graduate student, Dr. R. M L Baker (TSC), G.V. Stephenson (TSC)**. This is expected to require 10 to possibly 10,000W (1,000W nominal) at around 10GHz, with an associated power supply and appropriate safety interlocks. Possible technologies include solid-state, magnetron, traveling-wave tube (TWT), or high-power klystron, and specifications will be developed under this component of the work. These are all mature technologies and commercial units will suffice. Possible suppliers include: Microwave Power Inc. (Santa Clara, California; solid-state, up to 500W); ETM Electromatic Inc. (Newark, California; TWT or klystron, up to 10kW); and Toshiba Electron Tube and Devices Co., Ltd. (Japan; TWT or klystron, over 10kW). Generally speaking, wideband solid-state amplifiers produce less output power than medium bandwidth models or narrow-band tube designs, so that the compromise here will be to decide whether to accept lower power in favor of wide tunability. Also required is a suitably matched transmit antenna. Again, commercial designs will suffice, such as those from Rozendal Associates Inc. (Santee, California), ETS-Lindgren (Cedar Park, Texas), or Orban Microwave Products (El Paso, Texas). The compromise that must be worked out in the antenna design is that a high-gain antenna is needed to constrain the GB to be within the resonance cavity or interaction volume (so that microwave input power is not wasted), but a high-gain antenna is less tunable than a broadband low-gain antenna. As in other work areas of this proposal, the complete design will need to establish the cost-performance tradeoff issues surrounding the various approaches.

DD1.4 Fractal Membranes and Microwave Absorbers

Design of the fractal membranes as microwave reflectors/absorbers at select frequencies (Wen *et al.*, 2002; Zhou *et al.*, 2003) and other high-performance microwave absorbers: **Dr. R. M L Baker (TSC), G.V. Stephenson (TSC)**.

DD1.4.1 Design of the **fractal membrane (FM) reflectors** at the waist of the Gaussian beam including their paraboloidal form. An analysis will be completed to determine the optimal material of the FMs (copper, stainless steel, or aluminum are the obvious leading candidates). A paraboloidal surface will be designed that can be fabricated from the FM to focus the PPF at the planned locations of the microwave receivers. Hong Kong University of Science and Technology can fabricate the fractal membranes out of these metals in almost any form.

DD1.4.2 The **interior** of the containment vessel (except for an opening at the Gaussian-beam transmitter end) must be treated to eliminate exterior sources of noise. Either a Faraday Cage (using a mosaic of HTSC tiles; for example, YBCO) or fractal membranes are possibilities. Both will be examined in detail to determine the optimal approach. A design compatible with the containment vessel shape (DD1.1.4) and placement of interior detector elements will be developed.

DD1.4.3 Selection of appropriate microwave **absorbing material** at around 10GHz; design of the interior baffles around the Gaussian beam, and a "tunnel" between fractal-membrane reflectors and receivers (Baker, Stephenson and Li, 2008). A computer program for ray tracing of the PPF and the BFF will be developed and utilized for the baffle design. An analysis will be made of the latest technology reported by Chan *et al.* (2006), Landy *et al.* (2008), and Yang *et al.* (2008), and these will be compared with those available from established suppliers of current technology high performance microwave absorbing materials including ARC Technologies, Inc. (San Diego, California), Millimeter Wave Technology Inc. (Passaic, New Jersey), Cuming Microwave (Avon, Massachusetts), and many others.

DD1.5 Detection Receivers

Design of the microwave receivers (for the PPF) at each end of the detector containment vessel, tunable around 10GHz: **G.V. Stephenson (TSC), Dr. R.C. Woods (LSU) + graduate student, Dr. R. M L Baker (TSC)**. Three possibilities have already been identified for the technology to be used here, and specifications will be developed for each option found suitable for use in the final design so as to enable a final choice to be made.

DD1.5.1 Off-the-shelf microwave horn plus HEMT receiver: if tens to hundreds of photons per sample are available then standard microwave horns may be used, coupled to high electron mobility transistor (HEMT) amplifiers. This task will include a sensitivity analysis of this receiver type to determine the suitability of this approach, and a conceptual design will be developed using off-the-shelf components. Now highly developed, HEMT technology has previously been found reliable enough to use in the receivers for differential microwave radiometers (DMRs) flown in the NASA CDsmic Background Explorer (COBE) satellite mission.

DD1.5.2 Rydberg-Cavity Receiver as developed at Kyoto University (Yamamoto *et al.*, 2000)**:** Rydberg atoms are excited atoms with one or more electrons that have a much higher principal quantum number than ground state, usually conditioned *via* laser pumping. The low binding energy of the excited electrons leads to very low photoionization energy; therefore, Rydberg atoms are sensitive to low-energy microwave photons, and allow a microwave device somewhat analogous to a conventional photomultiplier tube to be constructed. When a microwave photon strikes a high cross-section Rydberg atom, it causes the electron to be ejected and the atom is ionized. If a large electric field is established within the container, the electron is accelerated, causing cascading impact ionization. The advantage of this receiver is that it is sensitive to low-energy single-photon events, and has very good time resolution. The disadvantage is its cost and complexity. This task will include a conceptual design of an alternative Rydberg atom receiver apparatus suitable for the PPF arising from HFRGW, and will also include a sensitivity calculation of the proposed apparatus.

DD1.5.3 Circuit QED microwave receiver as developed at Yale University (Schuster *et al.*,2007)**:** a third option will also be explored, the Circuit QED microwave photon receiver. A resonant co-planar waveguide, containing a Cooper Pair Box (CPB) in the center and delineated by Josephson junctions, define a photo-sensitive area in the center of the cavity. The cavity qubit energy levels shift when the cavity encounters a microwave photon. The advantage of this type of receiver is that it is very sensitive to individual photons and can integrate multiple photons over time. It has the

disadvantage that this device is of a unique design that is currently available only from Yale University, and is likely not to be exportable. This task will include developing a conceptual design using this alternative type of receiver for the PPF arising from HFRGW.

DD1.6 Cryogenic System

Specification and design of the cryogenic system refrigeration unit, required for low-temperature operation to obtain the best possible reduction in intrinsic thermal noise: **Dr. R.C. Woods (LSU) + graduate student, Dr. R. M L Baker (TSC), G.V. Stephenson (TSC)**. The required criterion is that the temperature T satisfies $kBT << \hbar\omega$ (where kB is Boltzmann's constant); that is, $T << \hbar\omega/kB \approx$ 480mK for detection at 10GHz. This condition is satisfied by the target temperature for the interaction volume $T <$ 48mK, which can be obtained using a common helium-dilution refrigerator. Then, the signal PPF will be significantly greater than the thermal photon flux. Cost/performance tradeoffs may also be important in this design, so that other possible economic solutions to receiver cooling will also be considered before finalizing the design.

DD1.6.1 Off-the-shelf cryogenic systems: a number of companies have developed ultra-low temperature systems (mK range) for a variety of applications. A common application is refrigeration of receivers as needed in the Li-Baker HFRGW detector. One possibility is the Oxford Instruments' KelvinoxMX range (see summary data attached) that appears to suit the present requirements subject to further evaluation of each model in the range. Other manufacturers to be investigated include Scientific Magnetics (UK), and Cryofab Inc. (Kenilworth, New Jersey).

DD1.6.2 Specifications for system best suited to the detector: specifications will be established for the selected cryogenic system. This will include cryogen level monitoring devices (for example, Oxford Instruments Intelligent Level Meter ILM200) for warning if the cooling fails.

DD1.7 Electromagnet

Development of the electromagnet specification needed to produce the required static magnetic field (up to 35T, ~3T nominal): **Dr. R.C. Woods (LSU) + graduate student, Dr. R. M L Baker (TSC), G.V. Stephenson (TSC)**. It is expected that a commercial design can be identified for this task. The chosen design will be capable of providing the requisite magnetic field at least over the interaction cavity volume in the containment vessel. Exceptional field-uniformity is not a particularly important issue in this application, though the GW interaction volume or cavity (roughly cylindrical, 6cm diameter and 30cm long) plus extra volume for the surrounding apparatus is somewhat larger than many other experimental applications require, and the required field is perpendicular to the cylindrical axis. Hence, one solution is that the final solenoid design must completely surround the cylindrical axis of the interaction volume perpendicular to the applied field. An alternative approach is to use two solenoids, one each side of the interaction volume, similar to the popular Helmholtz coil configuration. In a development of this, a number of small (~6cm diameter) solenoids could be stacked along the length of the interaction volume, with their Helmholtz-like opposite paired solenoids the other side of the interaction volume. In the latter cases, since the paired solenoids are not perfect ring coils, the resultant field would be non-uniform. A

quantitative estimate would be needed to ensure that the non-uniformity is not serious in the present application, but this is not expected to be a problem since field non-uniformity just produces non-uniform PPF generation in the interaction volume. The fractal membrane reflectors would still focus all the PPF at the receivers. The design tradeoff will be whether one or two large magnets are more cost-effective than a larger number of smaller magnets. The design effort will be divided into two major sub-tasks: off-the-shelf electromagnets currently available, and emerging-technology proposed magnets that may become available during the construction phase of the HFGW detector.

DD1.7.1 Off-the-shelf hardware: Excepting major installations, iron-core magnets are limited to around 2T over small volumes so that superconducting magnets are expected to be used here. Cryogen-free (more accurately, the cryogen is completely enclosed and re-cycled each time the magnet is cooled for use) superconducting magnets producing fields up to 16T are available commercially from a number of manufacturers including Scientific Magnetics, Oxford Instruments, and Cryogenic Ltd. (all UK). As examples, Oxford Instruments can supply magnets producing 9T in a 20cm bore, and 5T in a 1m bore. Typically, cooling is provided by an integral Gifford-McMahon cryo-cooler at 4.2K. Use of a cryogen-free "dry" magnet means that there are no cold seals to be a source of leaks.

DD1.7.2 Emerging technology: Since the detection PPF signal is directly proportional to the static magnetic field value, the detector sensitivity will be increased by using larger fields than currently-available commercial designs permit. To this end we will investigate the feasibility of co-developing with a third-party (for example, National High Magnetic Field Laboratory, Tallahassee, Florida) a custom-made high-field design capable of up to 35T (Bird, 2004), which may be realizable during the construction phase of the Li-Baker detector. If successful, achieving this value of magnetic field would improve the sensitivity of the Li-Baker detector by an order of magnitude. In this case, if a separate refrigeration system is required, the specification would include cryogen level-monitoring to ensure safe auto-rundown of the superconducting magnet if the helium level falls below a pre-set value, to reduce the danger associated with cryogenic-system related magnet failure. .l

Systems Engineering Tasks

Following the completion of the Li-Baker detector development tasks, plans and specifications will be drawn up by **LSU** in collaboration with **TSC**. Since overlap of tasks is possible, approximately 18 months will be allowed for the detector design, and approximately 8 months for the preparation of plans and specifications. With approximately two months overlap of the major tasks, a total of two years will be scheduled for the detector's design and development of the plans and specifications. Fig. 4.1a shows a Gannt chart for scheduling the project. For any large engineering project, coordination among investigators is important for the development of a coherent, unified design. This is the role of systems engineering tasks, depicted at the top of Fig. 4.1a. In the present case, the development of the detector will demand the close coordination of the detection link budget very early on, in order to carefully guide the component design for each of the component areas, and to ensure that the sensitivity goals can be met. This task culminates in a review of the predicted signal-to-noise ratio. A follow-on to this task is the development of key component requirements Interface requirements development is the next level of detail in systems engineering

task area, resulting in interface control documentation/drawing review prior to the critical design reviews of the component equipment areas. Finally, the systems engineering activity concludes with the development of test plans that will detail integration activities and reduce integration risk in subsequent phases. These activities are standard level-of-effort tasks that are rolled into other task bids as a background activity.

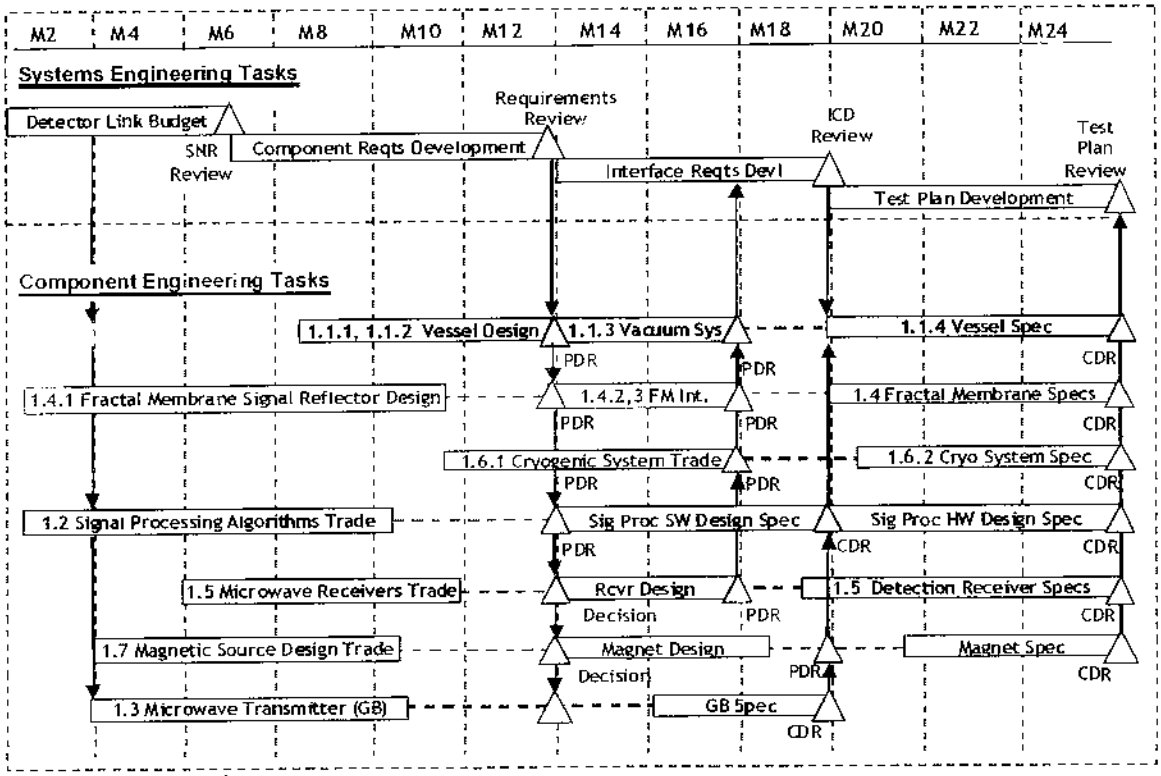

ICD = Interface Control Documentation/Drawing
PDR = Preliminary Design Review = design approval
CDR = Critical Design Review = design complete

Appendix C: Perturbative Photon Fluxes Generated By High-Frequency Gravitational Waves and Their Physical Effects